iScience

CellPress
OPEN ACCESS

Article

Notch and Delta Control the Switch and Formation of Camouflage Patterns in Caterpillars

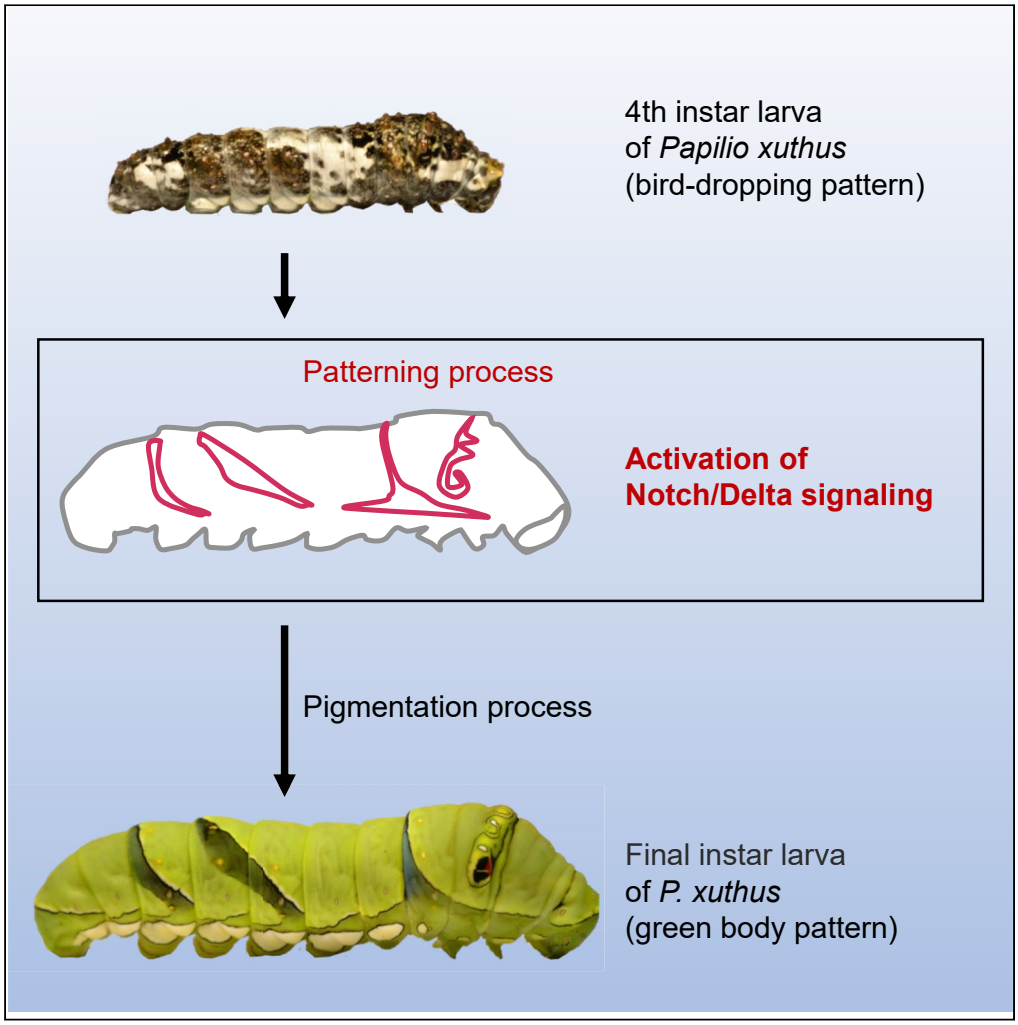

Hongyuan Jin, Shinichi Yoda, Liang Liu, Tetsuya Kojima, Haruhiko Fujiwara

haruh@edu.k.u-tokyo.ac.jp

HIGHLIGHTS

Notch and its ligand Delta regulate camouflage patterns of caterpillars

They define edge and pigmentation area in *Papilio xuthus* final larval patterns

They are suggested to bridge the juvenile hormone response period and final molt

Notch signaling pathway is important for caterpillars' color pattern evolution

Jin et al., iScience *23*, 101315
July 24, 2020
https://doi.org/10.1016/j.isci.2020.101315

iScience

CellPress
OPEN ACCESS

Article

Notch and Delta Control the Switch and Formation of Camouflage Patterns in Caterpillars

Hongyuan Jin,[1] Shinichi Yoda,[1] Liang Liu,[1] Tetsuya Kojima,[1] and Haruhiko Fujiwara[1,2,*]

SUMMARY

In most *Papilio* species, a younger larva mimics bird droppings but changes its pattern to match host plant colors in its final instar. This change is determined by juvenile hormone (JH) during the JH-sensitive period (JHSP) early in the fourth instar. Recently, we found that homeobox genes control the pre-pattern formation specifically during JHSP, but the molecular mechanisms underlying final patterning and pigmentation at molt are unknown. By knockdown of *Delta* and *Notch* in *Papilio xuthus* larvae, we here showed that these genes define the edge and pigmentation area in final patterns, during and even after JHSP, suggesting that they bridge the JHSP and molt. Knockdown of *Delta* in *Papilio machaon* led to similar phenotypic changes, and knockdown of *Notch* caused pigmentation loss in twin spots of the silkworm *Multilunar* (*L*) mutant. Our findings suggest the importance of the Notch signaling pathway in caterpillars' adaptive evolution of color pattern formation.

INTRODUCTION

Camouflage, mimicry, and aposematism, observed among many insects, are successful adaptive strategies to protect animals from predators (Bates, 1862; Caro et al., 2016; Cott, 1957; Poulton, 1890; Wallace, 1889). In most swallowtail butterflies in the genus *Papilio*, younger caterpillars show body coloration patterns that mimic bird droppings, which change during their final instar stage (Gaitonde et al., 2018; Igarashi, 1979). In the Asian swallowtail butterfly, *Papilio xuthus*, the younger larva (first–fourth instar stages) mimics bird droppings, with a black and white color pattern (mimetic pattern, Figure 1A) (Futahashi and Fujiwara, 2008; Prudic et al., 2007). However, the fifth instar larva switches to a cryptic greenish body, with a pair of eyespots and some dark green stripes, including a V-shaped marking across the abdominal 4 (A4) to 5 (A5) segments, which may help the caterpillar conceal itself in the host plant (Cryptic pattern, Figure 1A). Interestingly, the *Papilio* larva, such as *Papilio machaon* (the old-world swallowtail butterfly), which feeds on herbaceous or narrow-leaved plants (mainly umbellifers), shows a bold stripe in each segment in its final instar (Figure 1B). This pattern is totally different from that of other *Papilio* species, such as *P. xuthus*, which feeds on broad-leaved plants, such as citrus leaves (Gaitonde et al., 2018; Igarashi, 1979; Prudic et al., 2007). This phenomenon indicates that the color pattern of the final instar larvae has evolved to conceal them in the host plants (Caro et al., 2016), although the molecular mechanisms underlying these types of cryptic pattern formations are largely unknown.

Our previous study on *P. xuthus* showed that decreased titer of juvenile hormone (JH) during the early fourth instar stage (0–20 h after the third larval ecdysis) induced the larval coloration switch from the bird-dropping pattern to the host plant pattern (Figure 1C). This phase in early fourth instar stage is, thus, called the JH-sensitive period (JHSP). In contrast, that primitive group of these *Papilio* species (subgenus *Heraclides*) retains the bird-dropping phenotype throughout its larval life (Gaitonde et al., 2018; Igarashi, 1979; Prudic et al., 2007). This indicates that the JH-dependent pattern switch appeared later during the *Papilio* evolution. The pigmentation in the fifth instar larva occurs during the fourth molting stage (Futahashi and Fujiwara, 2007), about 3 days after the JHSP, according to the gene network orchestrated by 20-hydroxyecdysone (20E, known as the molting hormone) (Futahashi et al., 2010; Futahashi and Fujiwara, 2007) (Figure 1C). Thus, there is a 3-day gap between the two processes, i.e., the JH-dependent fate decision for the color switch and the actual execution of coloration by 20E, whereas the detailed molecular process during this time remains unclear.

To explore the molecular mechanisms underlying the JH-dependent color switch in *P. xuthus*, we recently carried out a transcriptome-wide screening for genes whose expression varies during the JHSP among

[1]Department of Integrated Biosciences, Graduate School of Frontier Sciences, The University of Tokyo, Kashiwa, Chiba 277-8562, Japan

[2]Lead Contact

*Correspondence: haruh@edu.k.u-tokyo.ac.jp

https://doi.org/10.1016/j.isci.2020.101315

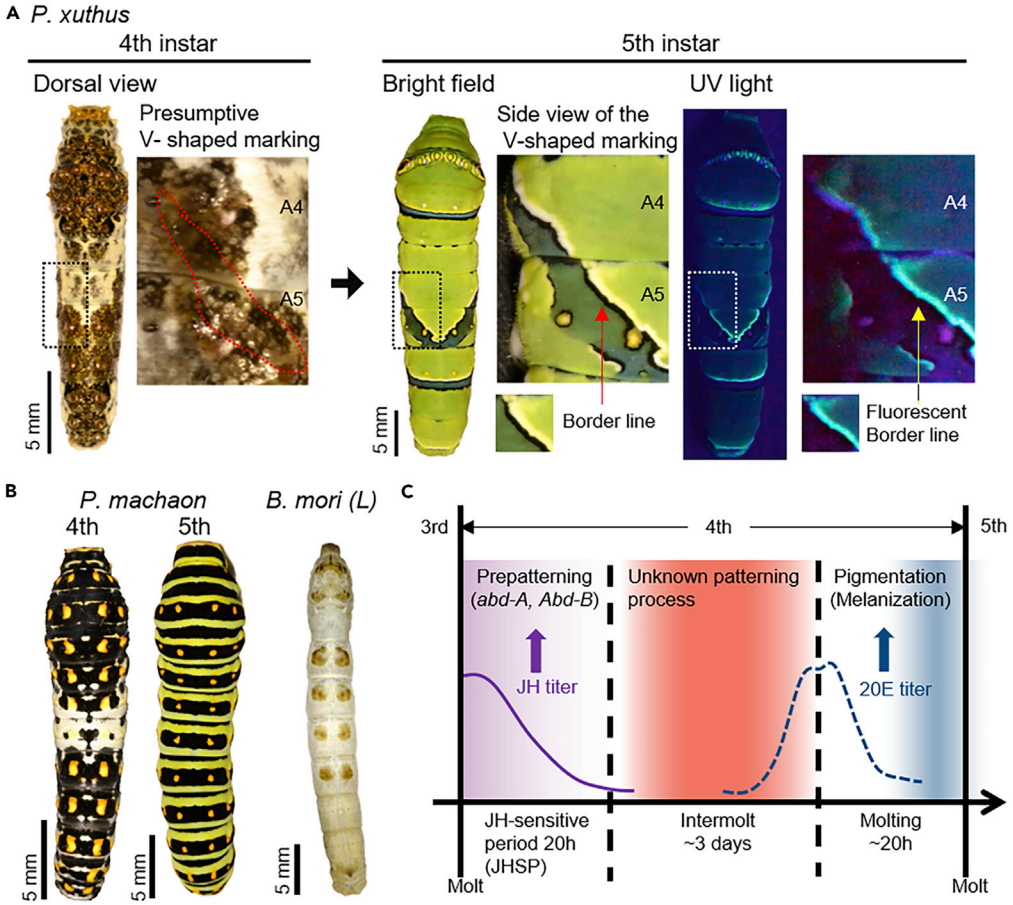

Figure 1. Color Pattern of Lepidopteran Caterpillars and a Schematic Diagram Showing Events during the Pattern Formation

(A) Dorsal view of fourth and fifth instar stage larvae of *P. xuthus*. Left panel, dorsal view of fourth instar larva showing body color pattern mimicking bird droppings. An enlarged side view with dashed red lines shows the presumptive V-shaped marking. A4 and A5: the fourth and fifth abdominal segments, respectively. Middle panel: a dorsal view of fifth stage larva with cryptic green body pattern. The enlarged side view shows the V-shaped marking in the black dashed box. The red arrow indicates the border line location, and a separate border line is displayed on the side of the arrow. Right panel: the color pattern of the fifth stage larva under UV light. The enlarged side view shows the fluorescent white line on the anterior side of the V-shaped marking. The yellow arrow indicates location of the white line, and a separate fluorescent border line is displayed on the side of the arrow. The dashed boxes indicate the enlarged regions of A4 and A5 under UV light, respectively. Scale bars: 5 mm.

(B) Fourth and fifth instar larvae of *P. machaon* and final instar larva of *B. mori* (*L* mutant).

(C) Schematic diagram of critical events and the underlying hormonal regulation. During the first 20 h of the fourth instar (JH sensitive period, JHSP), JH titer decline triggers the prepatterning process, including expression of *abd-A* and *Abd-B*. During the last 20 h of the fourth instar, a 20E-induced gene network regulates pigmentation and cuticle formation. The information on hormone changes was adapted and modified from Futahashi and Fujiwara (2008), and Futahashi et al. (2010).

different color pattern regions (Jin et al., 2019). Among the 20 candidates identified as the JH-regulated genes, we found that three homeobox genes, *clawless*, *abdominal-A* (*abd-A*), and *Abdominal-B* (*Abd-B*) are responsible for the final instar color patterning (Jin et al., 2019). Importantly, the final instar color patterning during the fourth molting period was inhibited by knockdown of these genes during the JHSP, but not afterward. This indicates that three homeobox genes function only during the JHSP; thus, we named these genes "prepatterning genes" (Figure 1C). However, the tightly regulated timing of these genes' functionality does not fully explain the developmental gap between JH-dependent fate decision and 20E-regulated pattern pigmentation, which motivated us to search for another type of gene bridging these two processes.

Among the 20 JH-regulated genes described earlier, *Delta*, encoding a specific ligand in the Notch signaling pathway, is of particular interest to us (Artavanis-Tsakonas et al., 1999; Fehon et al., 1990; Liao and Oates, 2017). The Delta ligand and the Notch signaling pathway are known to be involved in various types of cell-cell communication and cell patterning modulation during development (Artavanis-Tsakonas et al., 1999; Micchelli et al., 1997; Yoon and Gaiano, 2005). Therefore, we set out to investigate the functional role of *Delta* and the receptor gene *Notch* in the cryptic color formation, especially as bridging factors between the JH- and 20E-dependent processes. In this study, functional analyses, using electroporation-mediated RNA interference (RNAi) (Ando and Fujiwara, 2013), showed that *Delta* and *Notch*, but not the other ligand gene *Serrate* (Fleming et al., 1990), are involved in the formation of marking patterns in the fifth instar larval body in *P. xuthus*. Remarkably, knockdown of *Delta* and *Notch* partially disrupted the final instar larval patterning, even after the JHSP, indicating that these genes regulate patterning after the pre-patterning genes complete their roles, which contributes to progression from this stage into the fourth molting period.

To further determine whether the Notch signaling pathway's role in pattern formation during the larval stage is conserved among Lepidoptera, we studied their function in *P machaon*, which has a different type of final instar larval pattern, and the silkworm *Bombyx mori* mutant *Multilunar* (*L*), which shows twin spot markings in each segment (Figure 1B). Our results from *P. xuthus* and the other two species revealed an important function of the Notch signaling pathway in camouflaging pattern formation, which has evolved and diverged among the lepidopteran caterpillars.

RESULTS

Characteristics of V-Shaped Marking in the Fifth Instar Larval Stage of *P. xuthus*

In this study, we focused on the formation of the V-shaped marking, which could be seen on the dorsal side of the final instar larva of *P. xuthus* (Figure 1A). The marking lies across the fourth and fifth abdominal segments (A4 and A5) as a dark green stripe with two left-to-right symmetrical triangle patterns. Each half of the V-shaped marking is surrounded by two diagonal edges, one on the anterior and the other on the posterior side (Figure 1A). The anterior edge of the V-shaped marking consists of two lines, a white line adjacent to the green region and a black line next to the white line (Figure 1A). We named the set of white and black lines the "border line" of the V-shaped marking (Figure 1A, middle panel). Although the thin border line was observed consistently at the anterior edge, the black and white lines (in reverse orientation to anterior edge) appeared intermittently at the posterior edge. Interestingly, we noticed that the white line of the border absorbs UV light and emits florescent light (Figure 1A, right panel), which was, thus, used for phenotypic observation in RNAi analyses. In addition, the intersegmental color marking lines within the A1, A6, and A8 segments consist of white and black lines on the posterior side in each segment. Similar UV fluorescence was seen in the white lines of the dorsal side in the A1, A6, and A8 segments and inside the eyespot region of the T3 segment (Figure 1A, right panel).

Temporal and Spatial Expression Patterns of *Delta* and *Notch* during the JHSP

We previously identified *Delta* as a differentially expressed gene during the JHSP by RNA sequencing analysis (Jin et al., 2019). To understand *Delta's* role in larval coloration, we first analyzed its temporal and spatial expression patterns in the V-shaped marking and its surrounding regions during the JHSP (Figure 2, left panel). We prepared mRNA from the V-shaped marking (denoted as "V"), the eyespot region on the T3 segment (E), the dorsal region on A3 (D), the green region across A3-A4 (G), and the middle region across A3-A5 (M), at 0, 6, and 12 h after the third molt. Using quantitative polymerase chain reaction (qPCR), we compared *Delta's* expression patterns (Figure 2, right panel, *Delta*). Among all five regions, we found that the *Delta* expression level was significantly higher in the G region at 0 and 6 h (ANOVA, p value = 0.0010 and 0.0085, respectively), whereas its expression decreased during the JHSP (Figure 2). *Delta's* expression was relatively lower in the other four regions, although its expression levels in E and D regions were slightly higher than those in the M and V regions.

Different expression levels of Delta ligand activate the Notch receptor and downstream signaling pathway in various regions, which, in turn, induces *Notch* expression (Artavanis-Tsakonas et al., 1999; de Celis and Bray, 1997). To further ascertain whether expression of other factors in the Notch signaling pathway changes during formation of the V-shaped making, we analyzed genes encoding Notch and another ligand, Serrate (Fleming et al., 1990). *Notch* gene expression was detected in all five regions, with relatively constant levels in G and D regions, whereas their expression fluctuated during the JHSP in the remaining

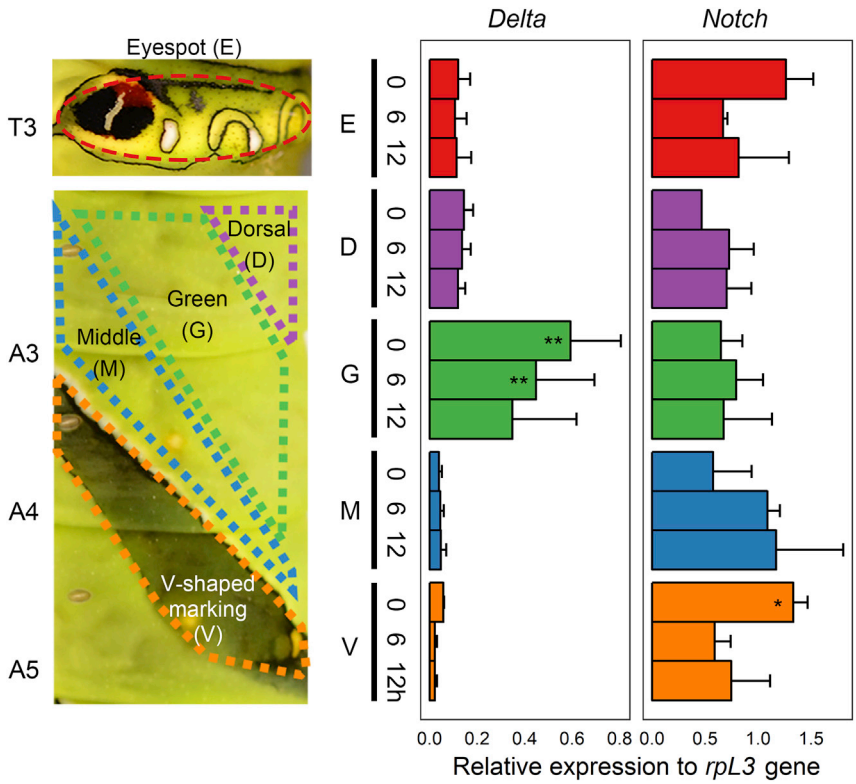

Figure 2. Temporal and Spatial Expression Patterns of *Delta* and *Notch*

Sampling regions for mRNA are shown on the left panel, from anterior to posterior of *P. xuthus* larva: the eyespot region (E) on T3 segment, the dorsal region (D) on A3 segment, the green region (G) on A3-A4 segments, the middle region (M) on A3-A4 segments, and the V-shaped marking (V) on A4-A5 segments. Relative expression levels are shown on the right panel and plotted as means + SD. Epidermis samples were prepared at 0, 6, and 12 h in the JHSP. Number of samples: n = 6 in E; n = 3 in D, M, and V; n = 9 (*Delta*) and 6 (*Notch*) in W. For statistical analysis, a one-way ANOVA, followed by a Tukey HSD test, was applied to analyze differential gene expression at the same time point among different sampling regions. For the *Delta* gene, the p value of 0 h group was 0.0010 and of 6 h group was 0.0085. For the *Notch* gene, the p value of 0 h group was 0.0325. *$p < 0.05$; **$p < 0.01$.

three regions (Figure 2, right panel, *Notch*). The *Serrate* gene expression pattern appeared similar to *Delta's*, showing higher expression in the G region than other regions (Figure S1). Further to know whether expressions of Notch pathway genes are affected by the JH titer, we have re-analyzed expression profiles of *Notch*, *Delta*, and *Serrate* based on the RNA-seq data obtained in our former report (Jin et al., 2019). After a JH analog (fenoxycarb) was applied on the fourth instar larvae just after the third molt, we prepared RNA samples from each region (E, G, and V) at 0, 6, and 12 h and performed RNA-seq analysis. Figure S2 shows the region-specific repression of three genes by the JH application: repression of *Delta* in the G and V regions; repression of *Serrate* in the G region; and repression of *Notch* in the E and V regions.

Repression of *Delta* Causes Ectopic V-shaped Marking in the Green Region

To further determine the Notch signaling pathway's function in color patterning of *P. xuthus* larva, we used a modified electroporation-mediated RNAi method (Ando and Fujiwara, 2013), which enabled us to knock down genes of interest in desired regions at specific developmental stages. Based on *Delta's* spatial expression, we reasoned that its imbalanced spatial expression may be involved in the V-shaped marking formation. Therefore, we introduced the *Delta* siRNA, through electroporation, during the late third instar stage (before head capsule slippage, HCS), and designed two types of experiments to test our hypothesis (Figure 3). In the type I experiment, we knocked down *Delta* in the green region (A3 to A4), resulting in an area with low *Delta* expression surrounded by areas with high *Delta* expression. In the type II experiment, we knocked down *Delta* in a wider area that covers both the green and future V-shaped marking (A4–A5) regions to observe the effect on the border line formation.

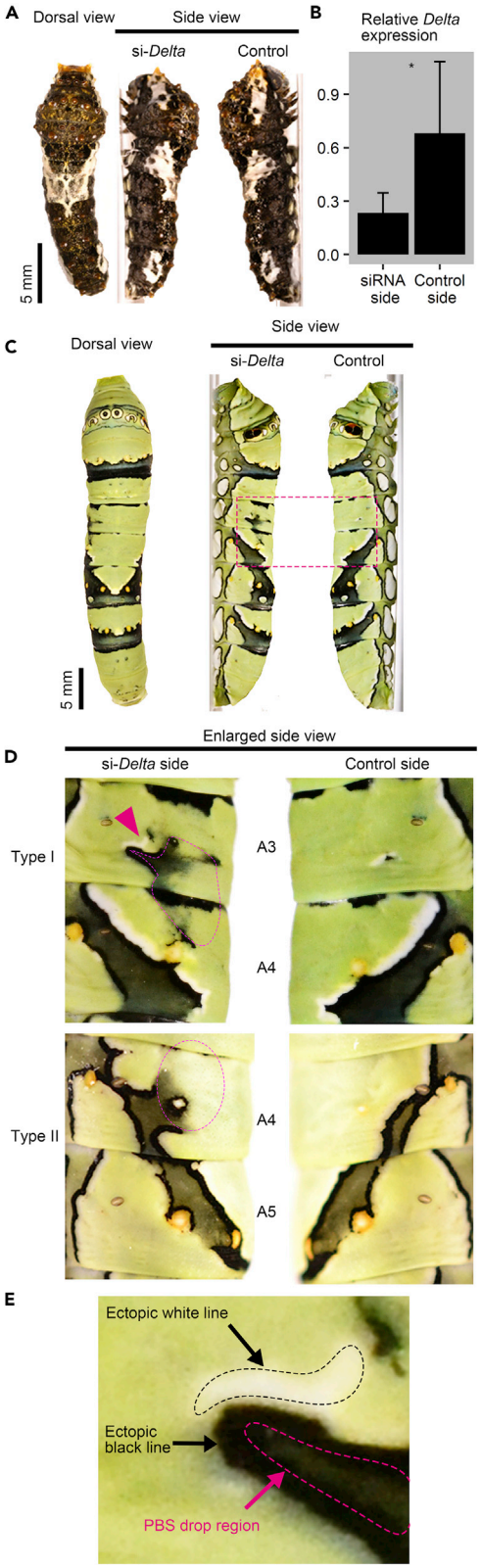
A
Dorsal view
Side view
si-Delta
Control
5 mm
B
Relative Delta expression
0.9
0.6
0.3
0.0
*
siRNA side
Control side
C
Dorsal view
Side view
si-Delta
Control
5 mm
D
Enlarged side view
si-Delta side
Control side
Type I
A3
A4
Type II
A4
A5
E
Ectopic white line
Ectopic black line
PBS drop region

Figure 3. Effect of *Delta* knockdown

Delta knockdown was performed during the late period of third instar of *P. xuthus*, and the results were observed at the fourth and fifth instar stages.

(A) No phenotypic changes were observed in fourth instar larva after *Delta* knockdown. *si-Delta*, siRNA-treated side; Control, non-treated side. Scale bar: 5 mm.

(B) Confirmation of effects of knockdown using qPCR. Relative expressions were plotted as means + SD. n = 5, Student's t test was performed, *p = 0.0313.

(C) The fifth instar larva after *Delta* knockdown in the green region (type I, see text). The dashed red box shows A3 and A4 segments. Scale bar: 5 mm.

(D) Enlarged phenotypic changes of type I (same individual as in C) and type II experiment (see text). The arrowhead indicates ectopic pigmentation and emergence of a newly formed border line. Scale bar: 5 mm. The dashed red circles represent the knockdown area (PBS droplet region, see text).

(E) Enlarged ectopic border in (D, Type I). Region with high *Delta* expression shows green coloration, whereas that with low *Delta* in the knockdown area shows dark green.

In all individuals treated with *Delta* siRNA, we found no phenotypic changes during the fourth instar stage (n = 11; Figures 3A and S3). We confirmed the siRNA knockdown results by qPCR using samples from the epidermis, dissected from both the siRNA-treated side and the untreated control side, at 12 h of the fourth instar stage. The results showed that *Delta* expression decreased significantly in the siRNA-treated side (Figure 3B, n = 5, Student's t test, p = 0.0313). However, most individuals (10/11, 90.9%) showed color pattern changes in the fifth instar stage (Figures 3C and S3). To ensure siRNA knockdown results are interpreted accurately, we included negative control siRNA and found no phenotypic changes in either fourth or fifth instar larvae in *P. xuthus* (Figures S4 and S5).

Moreover, in both type I and II experiments, ectopic black pigmentation appeared in the green region, but not in the control side, in the fifth instar stage after *Delta* knockdown (Figures 3D and S3). In those individuals in which *Delta* was knocked down in the green region (Type I), the V-shaped marking pattern, including the anterior border line (a set of white/black lines), dark green region, and posterior black line, appeared ectopically, with irregular shapes (Figures 3D and S3, type I). This result indicates that *Delta* regulates the entire V-shaped marking in the green region. To further analyze *Delta* knockdown's effects on border formation, we marked the siRNA knockdown region by tracing the positions of phosphate buffered saline (PBS) droplets on the side of the positive electrode (+side) during electroporation (represented by dotted red circles in each figure). By comparing the patterns of PBS droplets and ectopic pigmentation, we found that the black or white lines appeared at the edge of the PBS droplet area (Figure 3D, type I, red arrowhead; Figure 3E, an enlarged photo of 3D; Figure S3, type I), indicating that they are formed at the boundary between the area with *Delta* knockdown and normal *Delta* expression level. In contrast, the dark green region appeared inside the region of PBS droplets, which represents the *Delta* knockdown area. In some individuals, the *Delta* knockdown area (PBS droplet area) expanded from the green region to the original V-shaped marking area (Figures 3D and S3, Type II). We observed that the anterior border line of the V-shaped marking was broken and curved, and the black pigmentation extended from these V-shaped markings to the green region, presumably because of redistribution of *Delta* expression.

Notch Signaling Defines Border Lines in the Fifth Instar Larval Pattern

Because Delta is the specific ligand for Notch (Artavanis-Tsakonas et al., 1999), we next examined whether the *Notch* gene is involved in larval color pattern formation. The results from *Delta* RNAi knockdown suggest that the border line formation is related to the Notch signaling pathway activation; thus, we knocked down the expression of *Notch* via RNAi near the future V-shaped marking site (Figures 4 and S6) during the late third instar stage and examined the potential phenotypic change during the fourth and fifth instar stages. Similar to *Delta* knockdown, *Notch* knockdown in the V-shaped marking caused no color pattern change during the fourth instar stage (n = 10; Figures 4A and S6). Instead, it led to a dramatic alteration in color pattern in the fifth instar stage (n = 8; Figures 4C and S6). We confirmed that the *Notch* expression was highly repressed by siRNA using qPCR (Figure 4B, n = 3, p = 0.0544).

When *Notch* was knocked down in the original V-shaped marking region (Type II), both the anterior and posterior border lines of the V-shape marking were broken and/or dislocated at the fifth instar stage in most individuals (Figures 4C and S6, type II). Moreover, we observed that the dark green pigmentation expanded into the green region from A5 to A3 and A4 segments (Figure 4D, type II). In addition, as expected, *Notch* knockdown in the green region (type I) led to an ectopic V-shaped marking, including

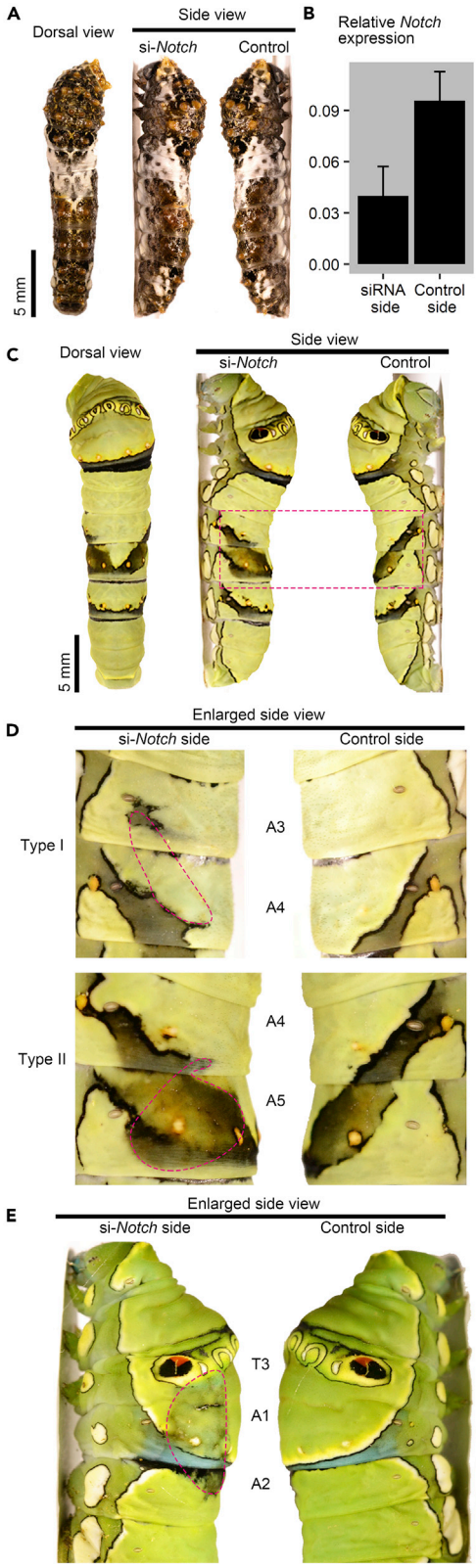
A
Dorsal view
Side view
si-Notch
Control
5 mm
B
Relative Notch expression
0.09
0.06
0.03
0.00
siRNA side
Control side
C
Dorsal view
Side view
si-Notch
Control
5 mm
D
Enlarged side view
si-Notch side
Control side
Type I
A3
A4
Type II
A4
A5
E
Enlarged side view
si-Notch side
Control side
T3
A1
A2

Figure 4. Effect of *Notch* Knockdown

Notch knockdown was performed during the late period of the third instar of *P. xuthus*, and the results were observed at the fourth and fifth instar stages.

(A) No phenotypic changes were seen in fourth instar larva after *Notch* knockdown. Scale bar: 5 mm.

(B) Confirmation of knockdown effects using qPCR. Relative expressions were plotted as means + SD. n = 3, Student's t test was performed, p = 0.0544. (C) The fifth instar larva after *Notch* knockdown around the V-shaped marking (type II, see text). The dashed red box shows A3 and A4 segments. Scale bar: 5 mm.

(D) Enlarged view of type I and type II (same individual as in **c**) experiments after *Notch* knockdown. The dashed red circles represent the knockdown area (PBS droplet region, see text). Ectopic and expanded pigmentation were observed in type I, but the border line disappeared in type II.

(E) Effect of *Notch* knockdown around the T3 to A2 segments.

the border lines and inner dark green pigmentation, a phenotypic change similar to that following *Delta* knockdown (Figures 4D and S6, type I).

In addition to the V-shaped marking, we have observed several border lines, including a set of white/black lines, at the anterior edge of a lateral blue band in A1 and the anterior edge of the lateral dark green band in A6 (Figure 1A). To determine *Notch*'s function in the border line formation in the whole larval body, we knocked down *Notch* in the border line between A1 and A2 of two larvae (Figure 4E). At the fifth instar stage, the A1-A2 border lines were broken, and the blue pigmentation between the two borders expanded into the T3 and A1 in both larvae (Figures 4E and S6). Interestingly the black lines around the eyespot region (T3) were also disrupted (Figure 4E). These results suggested that Notch defines the border line formation and that dislocation of *Delta* and *Notch* expressions alter the position and shape of V-shaped marking, A1-A2 border lines, and eyespot marking.

We also examined whether *Serrate* is involved in the larval color pattern formation by *Serrate* knockdown. We observed no phenotypic change in either the fourth or fifth instar larvae (Figure S7). These results indicate that among genes in the Notch signaling pathway, *Delta* and *Notch*, but not *Serrate*, regulate color pattern formation in the last instar larva of *P. xuthus*.

Function of *Delta* and *Notch* after JHSP

Our previous study revealed that the three prepatterning genes' function is restricted to the JHSP because knockdown of these genes after the JHSP had no effects on color pattern formation (Jin et al., 2019). To further understand how Delta and Notch contribute to color patterning, we performed RNAi knockdown of *Delta* and *Notch* after the JHSP during the fourth instar stage. We injected siRNAs for *Delta* or *Notch* at least 24 h after the third molt (at least 4 h beyond the JHSP) and confirmed gene expression knockdown using qPCR. Following both *Delta* and *Notch* knockdown, all the fifth instar larvae showed broken and diminished border lines around the V-shaped marking in the siRNA-treated side (Figures S8 and S9, bright field panel). However, we observed no effect on the pigmentation pattern of the V-shaped marking. To examine the phenotypic change of the border lines following RNAi treatment more closely, we placed individuals under ultraviolet (UV) light and recorded fluorescent signal emitted by the white lines (Figures S8 and S9, UV light panel). All individuals treated with *Delta* and *Notch* RNAi showed a partial depletion of the fluorescent signal in the border lines (Figures S8 and S9, UV light panel, pink arrowheads), consistent with the above observation. These results indicate that Delta and Notch modulate border line formation even after the JHSP, which is different from the previously reported prepatterning gene dynamics.

Function of the Notch Signaling Pathway in Larval Color Patterns of *P. machaon* and the Silkworm

To explore the Notch signaling pathway's function in regulating larval color patterns in other lepidopteran species, we carried out RNAi knockdown in *P. machaon*, a species closely related to *P. xuthus* (Figures 1B and 5A), and in a larval marking mutant *L* of the silkworm *B. mori* (Figures 1B and 5B), a species distantly related to *P. xuthus*.

Similar to *P. xuthus*, *P. machaon* changes its coloration pattern between the fourth and fifth instar larval stages, resulting in black stripes on the green body in each segment (Igarashi, 1979). When the *Delta* siRNA was injected around the A5 segment at the late third instar, there was no phenotypic change at the fourth instar stage (Figures 5A and S10). In the fifth instar stage, however, the anterior edge of the black stripe in A5 (Figure 5A, enlarged dorsal view; Figure S10) and A6 (Figure S10) expanded to the anterior side. In addition, thin black stripes appeared at the anterior edge of A5 (Figure 5A). However, no phenotypic change

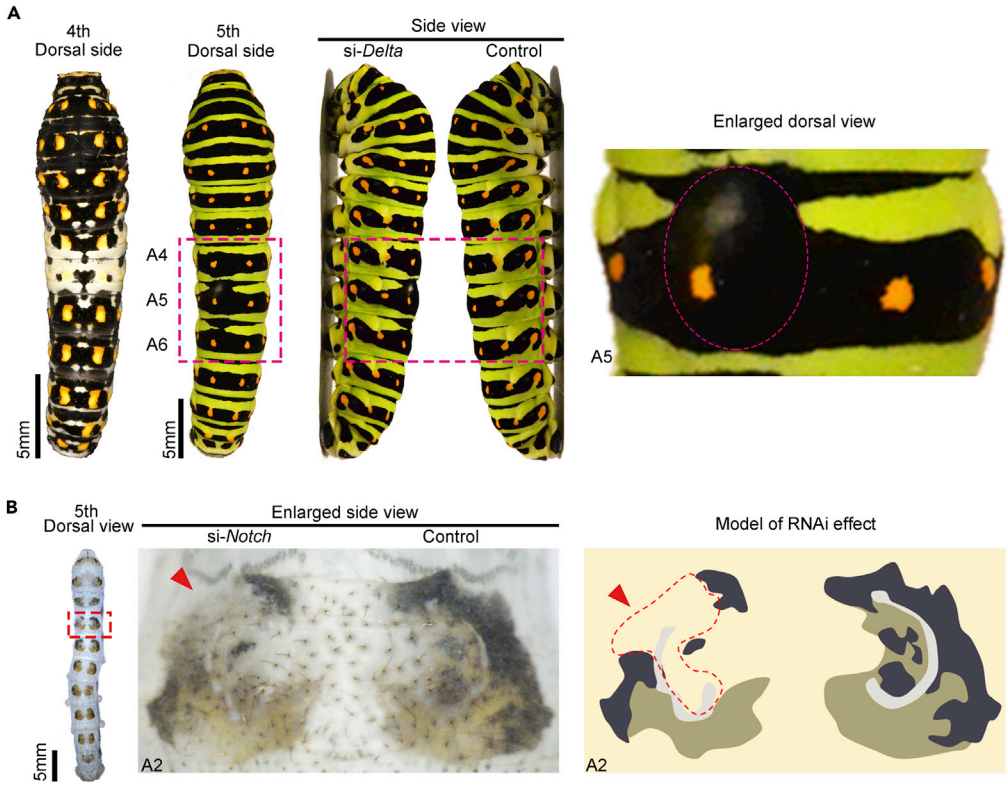

Figure 5. *Delta* Knockdown in *P. machaon* Larva and *Notch* Knockdown in *B. mori L* Mutant Larva

(A) The dashed red circles represent the *Delta* knockdown area in *P. machaon* larva. The effects were shown in fourth instar (left) and fifth instar larva (right). siRNA knockdown was performed at the last stage of the third instar larva. The red dashed box shows the A4-A6 segments. The enlarged dorsal view, on the right edge, shows that the black pigmentation expanded ahead after knockdown of *Delta* on A5. The dashed red circles represent the knockdown area. Scale bar: 5 mm.

(B) The effects of *Notch* knockdown on fifth instar larva of the *B. mori L* mutant. siRNA knockdown was performed at the late fourth instar stage, and the phenotypic change was observed at the fifth stage. The red arrowhead shows that black and brown pigmentation was depleted after *Notch* knockdown. The right panel represents a model (right) of *Notch* knockdown. In the knockdown area of *Notch* (indicated by dashed red circle), the melanin pigmentation disappeared. Scale bar: 5 mm.

was observed at the posterior edge of the black stripe (Figures 5A and S10). We concluded that *Delta* repression affected mainly the anterior part of black stripes in *P. machaon*, consistent with the results of *Delta* knockdown in *P. xuthus*.

We further examined the silkworm *L* mutant, which shows pairs of black brown twin spots on each larva body segment (Yamaguchi et al., 2013) (Figure 1B). It was reported that *Wnt1* (*wingless*) gene is responsible for *L* phenotype, and region-specific upregulation of *Wnt1* causes the twin spot markings (Yamaguchi et al., 2013). Unexpectedly, *Notch* knockdown in the twin spot region during the fourth instar stage caused loss of black pigmentation in the knockdown area (Figures 5B and S11). We also examined the functions of homologs of *Delta*, *Serrate*, and *fringe* genes (LeBon et al., 2014; Sato et al., 2008), which are critical factors in the Notch signaling pathway, in twin spot marking of the *L* mutant. The region-specific expression of these genes in *B. mori* (*L*) larva varies during the development and between regions (Figure S12). However, RNAi knockdown of *Delta*, *Serrate*, and *fringe* showed no effect on pigmentation or color patterning in the final instar larval stage.

In summary, these results indicate that the Notch signaling pathway regulates multiple larval color patterns among the distantly related lepidopteran species. Although the detailed mechanisms underlying hormonal regulation, color patterning, and pigmentation may differ and need to be studied further, the Notch signaling pathway serves as an evolutionarily conserved switch shaping the insect body color pattern and is used repeatedly through evolution for camouflage formation.

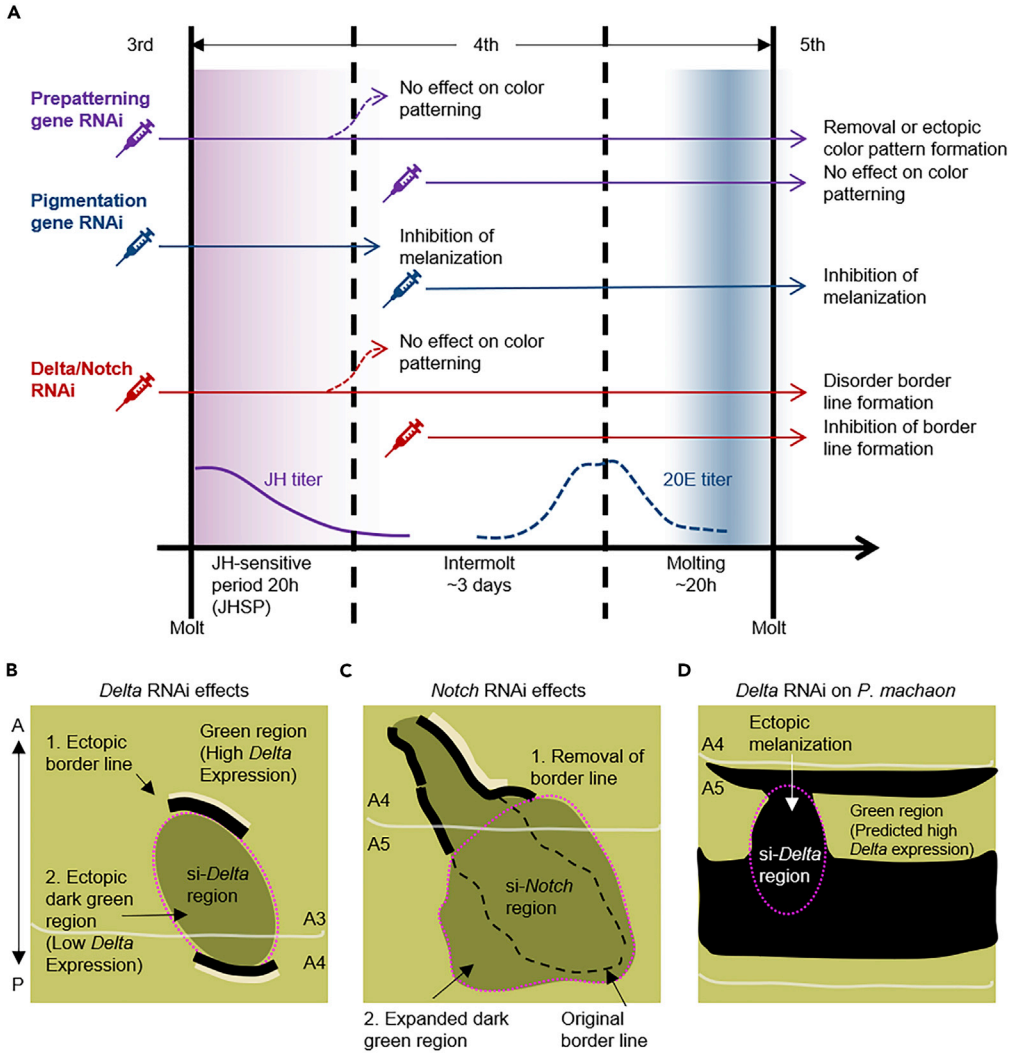

Figure 6. Effects of siRNA Knockdown and Genes Involved in Color Pattern Switch in *Papilio* Larva

(A) Three types of genes involved in the *P. xuthus* color pattern switch. Prepatterning genes (*cll*, *abd-A* and *Abd-B*) function only during the JHSP, whereas the pigmentation gene (*Laccase 2*) functions at every molting period (Jin et al., 2019). *Delta* and *Notch* function continuously throughout the JHSP and the intermolt of fourth instar, which is different from timing of activity of the prepatterning and pigmentation genes.

(B–D) The schematic diagrams show the phenotypic change after *Delta* knockdown (B) and *Notch* (C) in *P. xuthus* larva and *Delta* knockdown in *P. machaon* (D). (B) *Delta* knockdown results in low *Delta* expression area inside the dashed red circle, where the ectopic dark green coloration occurs (2). Between the green (higher *Delta* expression) and the dark green regions, border lines, consisting of a white and a black line, formed at both anterior and posterior sides (1). (C) *Notch* knockdown depletes border line (1) and expands dark green region (2), probably due to the disrupted *Delta* expression by *Notch* repression. The dashed red circle represents the *Notch* knockdown region. (D) *Delta* knockdown in *P. machaon* larva causes ectopic melanization and expansion of the black stripe area into the green region. The dashed red circle represents the *Delta* knockdown region.

DISCUSSION

In this study, we showed that *Delta* or *Notch* knockdown disrupted the coloration patterns of the final instar larva of *P. xuthus*, regardless of whether the siRNA was injected before or after the JHSP (Jin et al., 2019) (Figure 6A). This manner of gene action is different from that of other prepatterning genes, such as the *abd-A* and *Abd-b*, whose functions are limited to the JHSP (Figure 6A), or that of the downstream pigmentation gene, such as *Laccase 2*, which mediates the melanization process during every molting period (Futahashi and Fujiwara, 2007; Futahashi et al., 2011; Jin et al., 2019). *Delta* was previously reported to be upregulated

by reduced JH level in the green region (Jin et al., 2019), and expression of *Delta* and *Notch* was repressed by an increased JH level during the JHSP (Figure S2). Combining these JH-dependent expression reports with functional analyses, we reason that Delta and Notch activity initiate during the JHSP and continue, throughout the intermolt period (~3 days), until the molting period. Previously, we showed that knockdown of the prepatterning genes *abd-A* and *Abd-B* led to depletion or ectopic formation of the entire V-shaped marking (Jin et al., 2019) including the full set of border lines, which shares some similarity with the *Delta* and *Notch* knockdown results (Figures 3 and 4). Based on these observations, we concluded that the Notch signaling pathway transmits positional information for the final instar color pattern through the JHSP to the fourth molting. The Notch signaling pathway has been implicated previously in insect development, such as embryogenesis (Hoppe and Greenspan, 1986; Liao and Oates, 2017) and wing formation during metamorphosis (de Celis and Bray, 1997; Micchelli et al., 1997). However, our findings on Notch and Delta functions in larval color pattern formation provides new insights into how the local pattern change occurs at just one molting stage without changing whole body plan.

It is intriguing that Notch and Delta greatly impact the border line formation even after the JHSP. This may imply that the boundary information of color patterns is defined and maintained at later stages of color pattern switch (Figures 6B–6D). Notch's continuous activation is critical for cell adhesion (Bao, 2014), proliferation (Shimura et al., 2009), and other epidermal cell functions involved in color patterning. In conclusion, Notch and Delta determine more detailed shape and color of cryptic marking of the final instar stage, after the prepatterning genes initiate the regional information of cryptic color patterns during the JHSP (Figure 6A).

One important finding from the *Delta* knockdown is that the border lines of marking appeared between areas with decreased *Delta* expression and the surrounding areas with normal expression. This indicates that different *Delta* expression levels in adjacent regions initiates formation of the border line or the pigmentation area and defines their subsequent positions (Figure 6B). The Notch signaling pathway is known to be involved in cell-cell communication during development (Artavanis-Tsakonas et al., 1999; Bray, 2016; de Celis et al., 1998; Heitzler and Simpson, 1991; Liao and Oates, 2017; Micchelli et al., 1997), and its lateral inhibition results in different cell fates (del Alamo et al., 2011; Liao and Oates, 2017; Sprinzak et al., 2010). In the classic model, lateral inhibition occurs in a short range of neighboring cells (Heitzler and Simpson, 1991) because it requires direct contact between the Notch ligand and its receptor, both of which are transmembrane proteins. The border line formation in the adjacent regions following *Delta* (Figures 3D, 3E, and 6B) and *Notch* (Figures 4D and 6C) knockdown, therefore, is consistent with the lateral inhibition theory.

Furthermore, in the *Delta* knockdown experiment, it is intriguing that the entire V-shaped pattern appeared ectopically in the green region (Figure 3D, enlarged side view), with white and black lines in its anterior edge, the whole pigmented *Delta* knockdown area, and black and white lines in the posterior edge (in a reverse order to the anterior edge) (Figure 6B). The order of white/black lines in the ectopic marking is consistent with the original V-shaped marking, in which the white line always appears near the green region and the black line shows in neighboring dark green region. This indicates the ectopically created pattern still follows the anterior-posterior orientation of the larval segments, indicating that the Notch signaling pathway only regulates pigmentation pattern formation after the body plan has been determined. We observed some yellow spots located within and around V-shaped marking in *P. xuthus* (Futahashi et al., 2012) and within bold black stripes in *P. machaon* (Yamaguchi et al., 2013), which did not change following *Delta* knockdown (Figures 1 and 3D). Therefore, the Notch signaling does not affect formation of this spot, which was regulated by *Wnt1* in *P. machaon* (Yamaguchi et al., 2013). Moreover, the diagonal V-shaped marking exists across A3 to A5 segments, although the detailed mechanism underlying this intersegmental color pattern is unknown. One possible explanation is that the Notch-Delta pathway is modulated in a head-to-tail direction across the entire body, presumably by a morphogenic element such as Wnt (Collu et al., 2014; Sonnen et al., 2018).

The *Notch* expression pattern corresponded to the eyespot and midline color pattern in wings of the nymphalid butterflies (Reed and Serfas, 2004). Furthermore, in *Papilio polytes*, the *enhancer of split* gene, which is downstream to the Notch signaling pathway (Bailey and Posakony, 1995; Bray, 2006), showed a specific spatial-temporal expression patterns across wings (Iijima et al., 2019). By knockdown experiments in three species, however, the present study revealed more clearly the functional roles of the Notch signaling pathway in regulating the coloration pattern.

Moreover, we found that *Delta* knockdown in *P. machaon* disrupted the edge line formation of the bold stripe and induced black pigmentation in the siRNA-treated region (Figures 5A and 6D), similar to the results in *P. xuthus*. These two *Papilio* species are closely related (Zakharov et al., 2004), with similar changes between the younger mimetic pattern and the final instar cryptic pattern (Shirataki et al., 2010), which helps them camouflage in different types of host plants (Prudic et al., 2007). This indicates that *P. machaon* also has the JHSP in the early fourth instar stage and retains a similar pattern switch mechanism. The mechanism of JH-dependent pattern switch is conserved among many *Papilio* species and has diverged from the ancestral group, which retains the bird-dropping pattern throughout life (Prudic et al., 2007). Although the reason why the switch mechanism has diverged remains unknown, it is speculated that coloration mimicking the host plant is more effective than the bird-dropping pattern for protection from predators because the size of the last instar larva in the *Papilio* species usually exceeds 5 cm.

On the other hand, the knockdown of *Notch*, but not *Delta*, caused loss of the larval spot marking in the *L* mutant of *B. mori*, which is distantly related to *P. xuthus* (Figure 5B). This phenotypic change is opposite to the appearance of pigments in the knockdown area of *Delta* or *Notch* in *P. xuthus*. In addition, knockdown of neither *Serrate* nor *fringe* affected the pigmentation in the *L* spot (data not shown). Notch pathway involved in the larval pattern formation is conserved in Lepidoptera, although its gene network may be different among species. Because the twin spots of the *L* mutant are known to be caused by 20E-induced *Wnt1* expression (Yamaguchi et al., 2013), it is conceivable that the Notch signaling pathway regulates *Wnt1* expression in spot formation. It is known that the melanin synthesis in the larval epidermis occurs during the molting period under the control of the ecdysone cascade (Hiruma and Riddiford, 2009; Yamaguchi et al., 2013). Thus, the Notch signaling pathway involved in the pigmentation process of three species should be interacted closely with the 20E-induced gene pathway (Futahashi and Fujiwara, 2007; Futahashi et al., 2012).

Our findings shed new light on the Notch signaling pathway's function in the camouflage color formation of lepidopteran larva, thereby bridging two important development programs, the JH-dependent patterning and 20E-regulated pigmentation.

Limitations of the Study

Although we observed fluorescence emitting from the white lines in the V-shaped marking in caterpillar of *P. xuthus*, its biological function is unclear. Thus, a future study will be important to understand the molecular basis underlying synthesis of the fluorescent pigment in caterpillars of butterfly and moth.

Resource Availability

Lead Contact

Further information and requests for resources and reagents should be directed to and will be fulfilled by the Lead Contact, Haruhiko Fujiwara (haruh@edu.k.u-tokyo.ac.jp).

Materials Availability

This study did not generate new unique reagents.

Data and Code Availability

The published article includes all data generated or analyzed during this study.

METHODS

All methods can be found in the accompanying Transparent Methods supplemental file.

SUPPLEMENTAL INFORMATION

Supplemental Information can be found online at https://doi.org/10.1016/j.isci.2020.101315.

ACKNOWLEDGMENTS

We thank S. Shimizu for providing *P. xuthus* eggs and Y. Banno (Kyushu University, Japan) for providing *B. mori* larvae. We appreciate Drs. R. Tajiri, J. Yamaguchi, and S. Komata for giving critical suggestions on this manuscript. This work was supported by the Japan Society for the Promotion of Science (JSPS) Grants-in

Aid for Scientific Research (KAKENHI) from the Ministry of Education, Culture, Sports, Science, and Technology of Japan [MEXT/JSPS KAKENHI (20017007, 22128005, 15H05778, 18H04880, 16H06279) to H.F].

AUTHOR CONTRIBUTIONS

H. J. and H. F. designed the experiments. H. J., S. Y., L. L., T. K., and H. F. discussed and wrote the manuscript. H. J. performed the experiment and collected the data and visualized the figures. H.F. supervised the project.

DECLARATION OF INTERESTS

The authors declare no competing interests.

Received: March 27, 2020
Revised: May 21, 2020
Accepted: June 20, 2020
Published: July 24, 2020

REFERENCES

Ando, T., and Fujiwara, H. (2013). Electroporation-mediated somatic transgenesis for rapid functional analysis in insects. Development *140*, 454–458.

Artavanis-Tsakonas, S., Rand, M.D., and Lake, R.J. (1999). Notch signaling: cell fate control and signal integration in development. Science *284*, 770–776.

Bailey, A.M., and Posakony, J.W. (1995). Suppressor of hairless directly activates transcription of enhancer of split complex genes in response to Notch receptor activity. Genes. Dev. *9*, 2609–2622.

Bao, S. (2014). Notch controls cell adhesion in the Drosophila eye. PLoS Genet. *10*, e1004087.

Bates, H.W. (1862). XXXII. Contributions to an insect fauna of the Amazon valley. Lepidoptera: Heliconida. Trans. Linn. Soc. Lond. *23*, 495–566.

Bray, S.J. (2006). Notch signalling: a simple pathway becomes complex. Nat. Rev. Mol. Cell Biol. *7*, 678–689.

Bray, S.J. (2016). Notch signalling in context. Nat. Rev. Mol. Cell Biol. *17*, 722–735.

Caro, T., Sherratt, T.N., and Stevens, M. (2016). The ecology of multiple colour defences. Evol. Ecol. *30*, 797–809.

Collu, G.M., Hidalgo-Sastre, A., and Brennan, K. (2014). Wnt-Notch signalling crosstalk in development and disease. Cell. Mol. Life Sci. *71*, 3553–3567.

Cott, H.B. (1957). Adaptive Coloration in Animals, Repr. With Minor Corrections Edition (Methuen).

de Celis, J.F., and Bray, S. (1997). Feed-back mechanisms affecting Notch activation at the dorsoventral boundary in the Drosophila wing. Development *124*, 3241–3251.

de Celis, J.F., Tyler, D.M., de Celis, J., and Bray, S.J. (1998). Notch signalling mediates segmentation of the Drosophila leg. Development *125*, 4617–4626.

del Alamo, D., Rouault, H., and Schweisguth, F. (2011). Mechanism and significance of cis-inhibition in Notch signalling. Curr. Biol. *21*, R40–R47.

Fehon, R.G., Kooh, P.J., Rebay, I., Regan, C.L., Xu, T., Muskavitch, M.A., and Artavanis-Tsakonas, S. (1990). Molecular interactions between the protein products of the neurogenic loci Notch and Delta, two EGF-homologous genes in Drosophila. Cell *61*, 523–534.

Fleming, R.J., Scottgale, T.N., Diederich, R.J., and Artavanis-Tsakonas, S. (1990). The gene Serrate encodes a putative EGF-like transmembrane protein essential for proper ectodermal development in Drosophila melanogaster. Genes. Dev. *4*, 2188–2201.

Futahashi, R., Banno, Y., and Fujiwara, H. (2010). Caterpillar color patterns are determined by a two-phase melanin gene prepatterning process: new evidence from tan and laccase2. Evol. Dev. *12*, 157–167.

Futahashi, R., and Fujiwara, H. (2007). Regulation of 20-hydroxyecdysone on the larval pigmentation and the expression of melanin synthesis enzymes and yellow gene of the swallowtail butterfly, Papilio xuthus. Insect Biochem. Mol. Biol. *37*, 855–864.

Futahashi, R., and Fujiwara, H. (2008). Juvenile hormone regulates butterfly larval pattern switches. Science *319*, 1061.

Futahashi, R., Shirataki, H., Narita, T., Mita, K., and Fujiwara, H. (2012). Comprehensive microarray-based analysis for stage-specific larval camouflage pattern-associated genes in the swallowtail butterfly, Papilio xuthus. BMC Biol. *10*, 46.

Futahashi, R., Tanaka, K., Matsuura, Y., Tanahashi, M., Kikuchi, Y., and Fukatsu, T. (2011). Laccase2 is required for cuticular pigmentation in stinkbugs. Insect Biochem. Mol. Biol. *41*, 191–196.

Gaitonde, N., Joshi, J., and Kunte, K. (2018). Evolution of ontogenic change in color defenses of swallowtail butterflies. Ecol. Evol. *8*, 9751–9763.

Heitzler, P., and Simpson, P. (1991). The choice of cell fate in the epidermis of Drosophila. Cell *64*, 1083–1092.

Hiruma, K., and Riddiford, L.M. (2009). The molecular mechanisms of cuticular melanization: the ecdysone cascade leading to dopa decarboxylase expression in Manduca sexta. Insect Biochem. Mol. Biol. *39*, 245–253.

Hoppe, P.E., and Greenspan, R.J. (1986). Local function of the Notch gene for embryonic ectodermal pathway choice in Drosophila. Cell *46*, 773–783.

Igarashi, S. (1979). Papilionidae and Their Early Stages (Kodansha).

Iijima, T., Yoda, S., and Fujiwara, H. (2019). The mimetic wing pattern of Papilio polytes butterflies is regulated by a doublesex-orchestrated gene network. Commun. Biol. *2*, 257.

Jin, H., Seki, T., Yamaguchi, J., and Fujiwara, H. (2019). Prepatterning of Papilio xuthus caterpillar camouflage is controlled by three homeobox genes: clawless, abdominal-A, and Abdominal-B. Sci. Adv. *5*, eaav7569.

LeBon, L., Lee, T.V., Sprinzak, D., Jafar-Nejad, H., and Elowitz, M.B. (2014). Fringe proteins modulate Notch-ligand cis and trans interactions to specify signaling states. Elife *3*, e02950.

Liao, B.K., and Oates, A.C. (2017). Delta-Notch signalling in segmentation. Arthropod Struct. Dev. *46*, 429–447.

Micchelli, C.A., Rulifson, E.J., and Blair, S.S. (1997). The function and regulation of cut expression on the wing margin of Drosophila: Notch, Wingless and a dominant negative role for Delta and Serrate. Development *124*, 1485–1495.

Poulton, E.B. (1890). The Colours of Animals, Their Meaning and Use, Especially Considered in the Case of Insects (D. Appleton and Company).

Prudic, K.L., Oliver, J.C., and Sperling, F.A. (2007). The signal environment is more important than diet or chemical specialization in the evolution of

warning coloration. Proc. Natl. Acad. Sci. U S A *104*, 19381–19386.

Reed, R.D., and Serfas, M.S. (2004). Butterfly wing pattern evolution is associated with changes in a Notch/Distal-less temporal pattern formation process. Curr. Biol. *14*, 1159–1166.

Sato, K., Matsunaga, T.M., Futahashi, R., Kojima, T., Mita, K., Banno, Y., and Fujiwara, H. (2008). Positional cloning of a Bombyx wingless locus flugellos (fl) reveals a crucial role for fringe that is specific for wing morphogenesis. Genetics *179*, 875–885.

Shimura, S., Kiuchi, M., and Kiguchi, K. (2009). Spatial and temporal changes of mitotic activity in the epidermis during larval development of the silkworm, Bombyx mori. J. Insect Biotechnol. Sericol. *78*, 155–163.

Shirataki, H., Futahashi, R., and Fujiwara, H. (2010). Species-specific coordinated gene expression and trans-regulation of larval color pattern in three swallowtail butterflies. Evol. Dev. *12*, 305–314.

Sonnen, K.F., Lauschke, V.M., Uraji, J., Falk, H.J., Petersen, Y., Funk, M.C., Beaupeux, M., Francois, P., Merten, C.A., and Aulehla, A. (2018). Modulation of phase shift between Wnt and Notch signaling oscillations controls mesoderm segmentation. Cell *172*, 1079–1090 e1012.

Sprinzak, D., Lakhanpal, A., Lebon, L., Santat, L.A., Fontes, M.E., Anderson, G.A., Garcia-Ojalvo, J., and Elowitz, M.B. (2010). Cis-interactions between Notch and Delta generate mutually exclusive signalling states. Nature *465*, 86–90.

Wallace, A.R. (1889). Darwinism: An Exposition of the Theory of Natural Selection, with Some of its Applications (Macmillan).

Yamaguchi, J., Banno, Y., Mita, K., Yamamoto, K., Ando, T., and Fujiwara, H. (2013). Periodic Wnt1 expression in response to ecdysteroid generates twin-spot markings on caterpillars. Nat. Commun. *4*, 1857.

Yoon, K., and Gaiano, N. (2005). Notch signaling in the mammalian central nervous system: insights from mouse mutants. Nat. Neurosci. *8*, 709–715.

Zakharov, E.V., Caterino, M.S., and Sperling, F.A. (2004). Molecular phylogeny, historical biogeography, and divergence time estimates for swallowtail butterflies of the genus Papilio (Lepidoptera: Papilionidae). Syst. Biol. *53*, 193–215.

iScience, Volume *23*

Supplemental Information

Notch and Delta Control the Switch and Formation of Camouflage Patterns in Caterpillars

Hongyuan Jin, Shinichi Yoda, Liang Liu, Tetsuya Kojima, and Haruhiko Fujiwara

Supplemental Figures

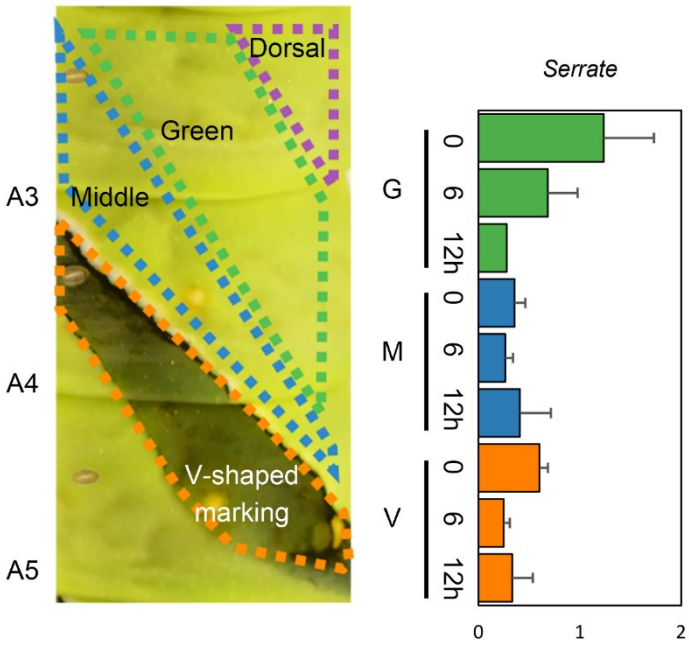

Figure S1. Relative expression pattern of *Serrate* gene in JH sensitive period, related to Figure 2. Data are represented as mean + s.d. *rpL3* gene was used as internal control. Color pattern was presented in "G" the green region, "M" the middle region, "V" the V-shaped region. 0, 6, 12 h indicated the time after the 3rd ecdysis. A3, A4, A5 showed the 3rd, 4th and 5th abdominal segment.

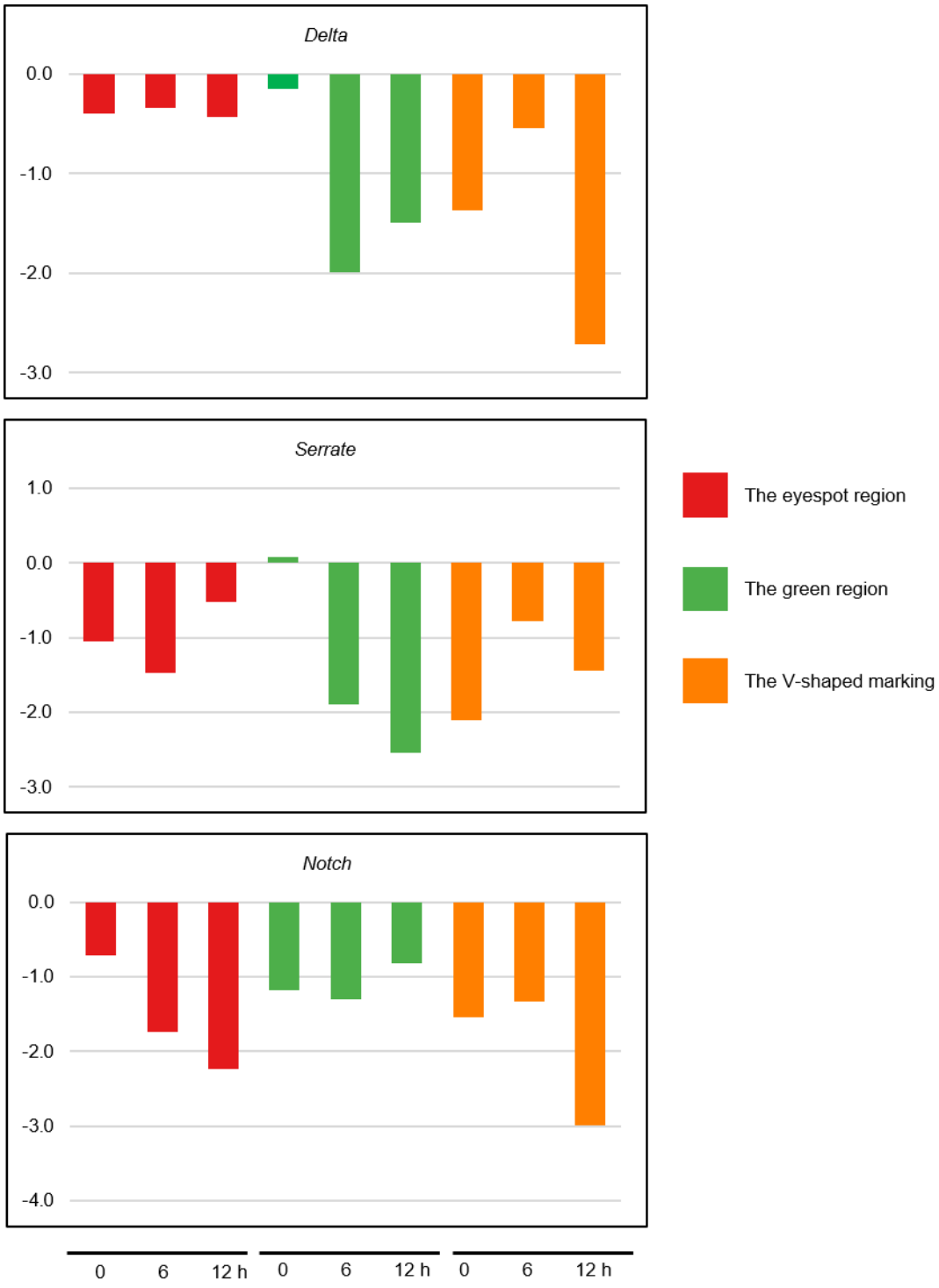

Figure S2. Expression change of *Delta*, *Serrate*, and *Notch* gene after JH analog application, related to Figure 2. Log 2 fold change was shown using RPKM from previous RNA sequencing experiment. Log 2 fold change was calculated as Log 2 (average RPKM of JH application group (n=2) / control group RPKM. All three genes were down-regulated by application of JH analog (5μg fenoxycarb immediately after the 3rd molt).

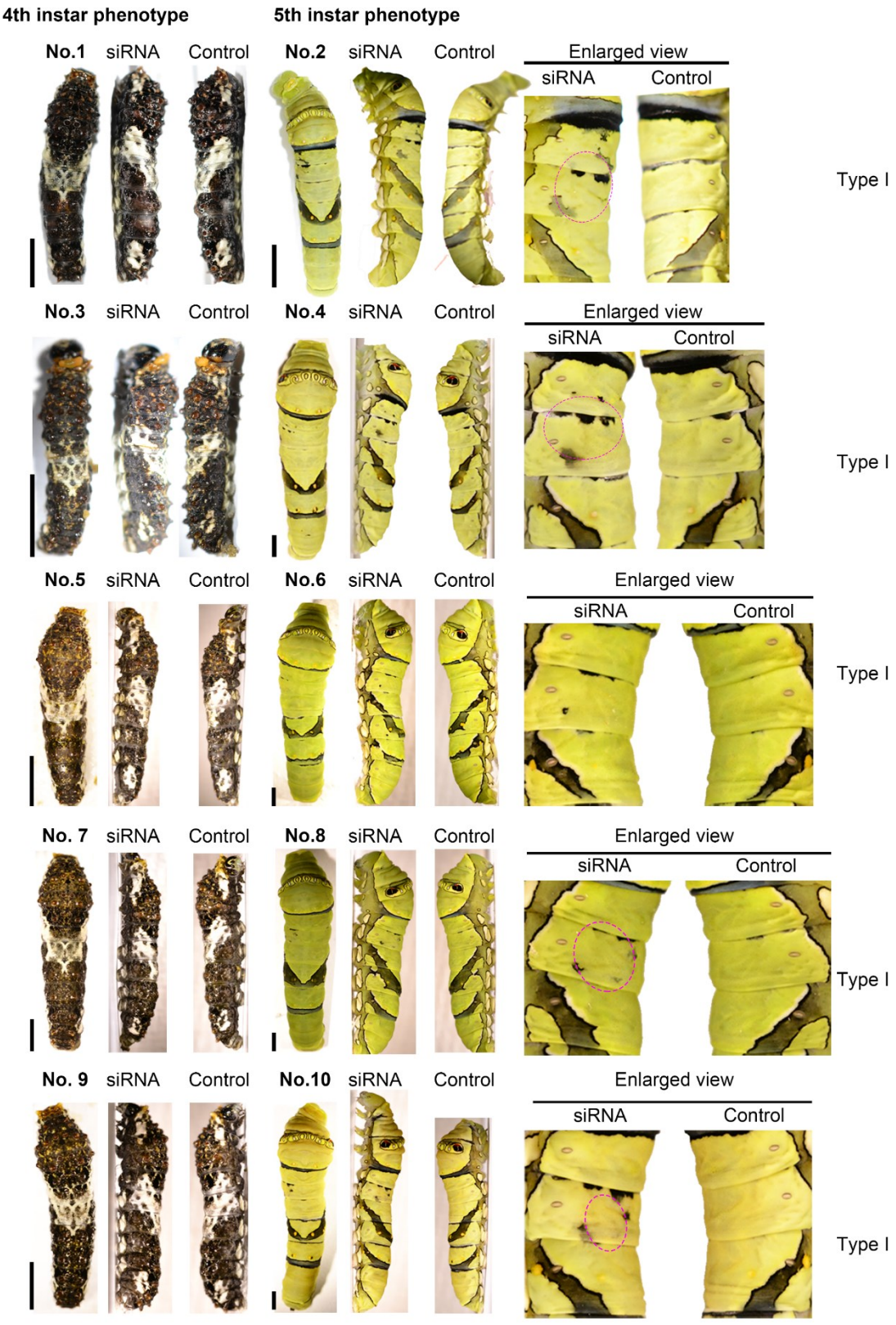

Figure S3. RNAi effects of *Delta*, related to Figure 3. Delta siRNA was injected at the 3rd instar stage and observed at 4th and 5th stage. The type I means that the PSB drop (RNAi region) was placed in the green area around A3 and A4. The type II means that the PSB drop (RNAi region) was placed around the future V-shaped marking around A3 to A5. Pink dashed circle shows the RNAi region. Scale bar: 5 mm

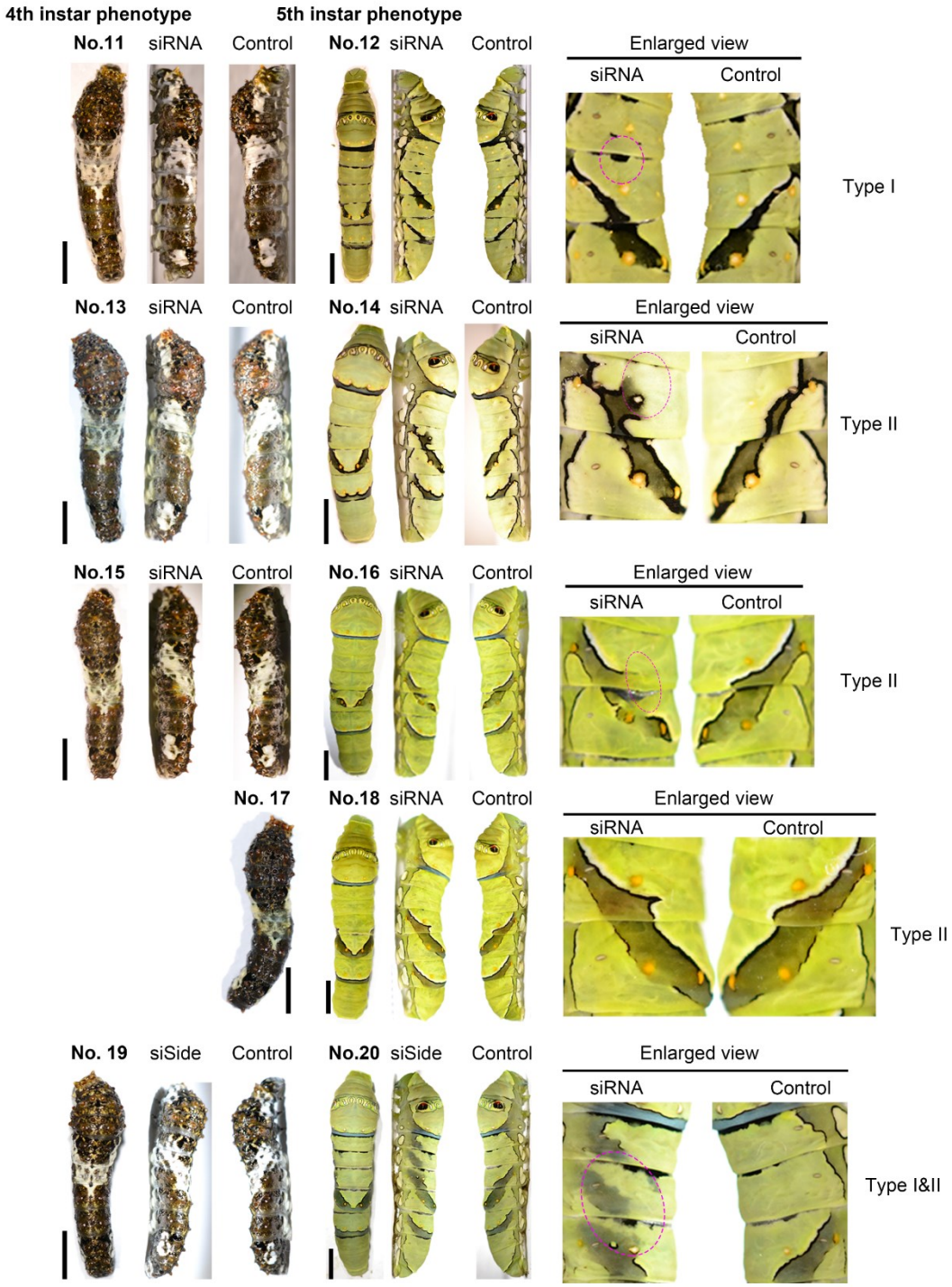

Continued Figure S3. RNAi effects of *Delta*, related to Figure 3.

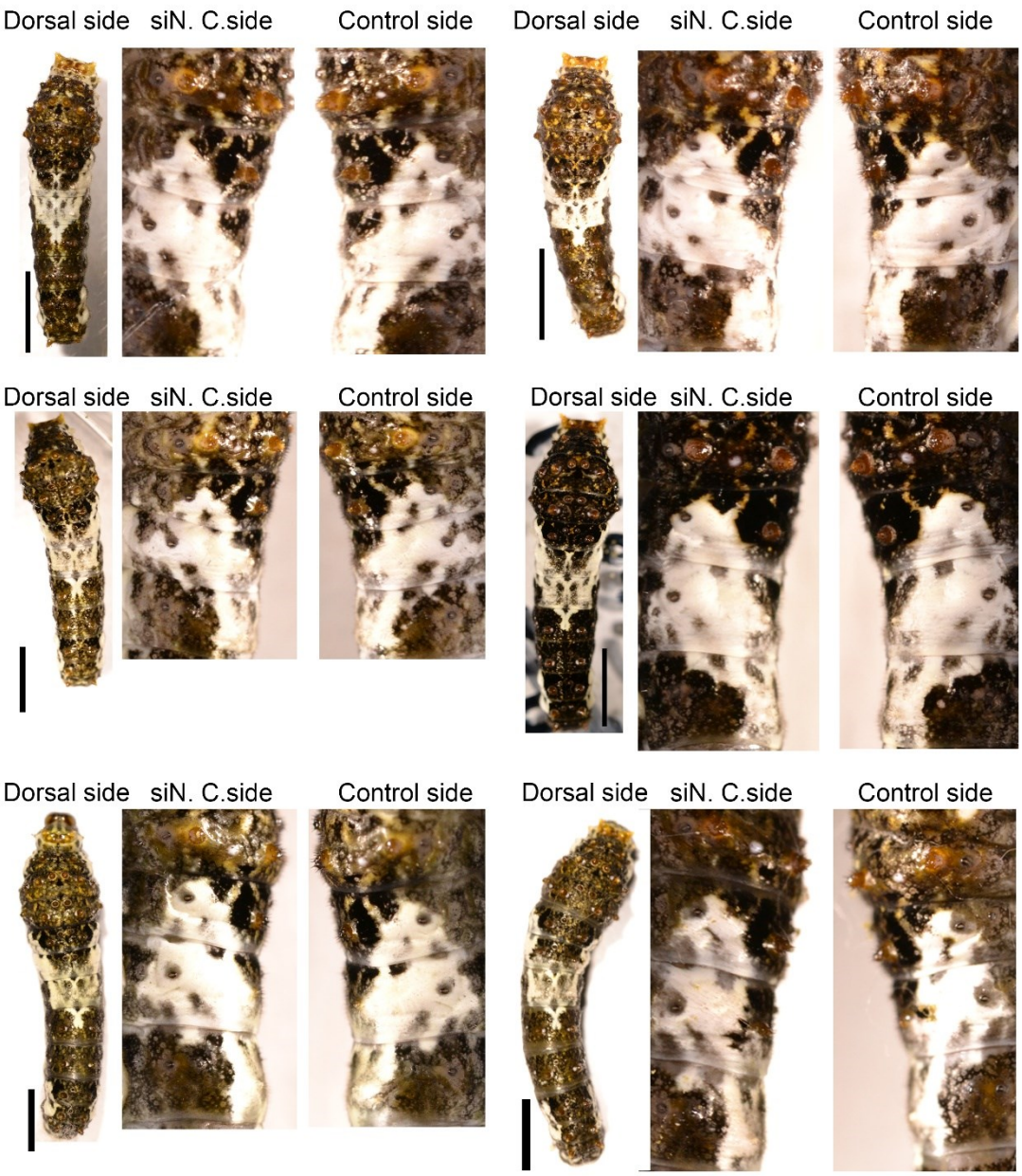

Figure S4. Effects of RNAi negative control on 4th instar larval of *P. xuthus*, related to Figure 3 and 4. No effects of negative control siRNA were observed on *P. xuthus* larvae. Injection was performed in six individuals by electroporation during the late 3rd instar stage, and results were observed at 4th stage. siRNA knockdown was performed in the 3rd to 4th abdominal segments. Scale bar: 5mm.

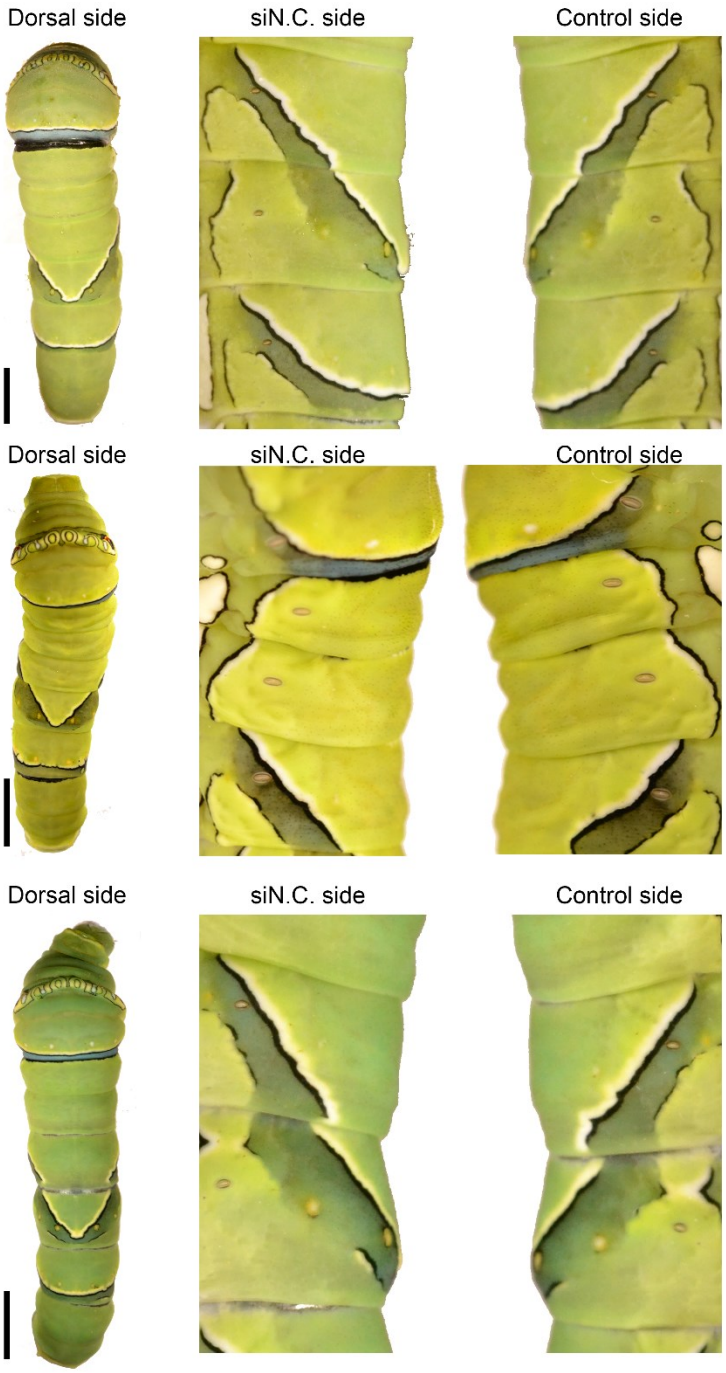

Figure S5. Effects of RNAi negative control on 5th instar larval of *P. xuthus*, related to Figure 3 and 4. No effects of negative control siRNA were observed on *P. xuthus* larvae. Injection was performed in three individuals by electroporation during the late 3rd instar stage, and results were observed at 5th stage. siRNA knockdown was performed in the 3rd to 4th abdominal segments. Scale bar: 5mm.

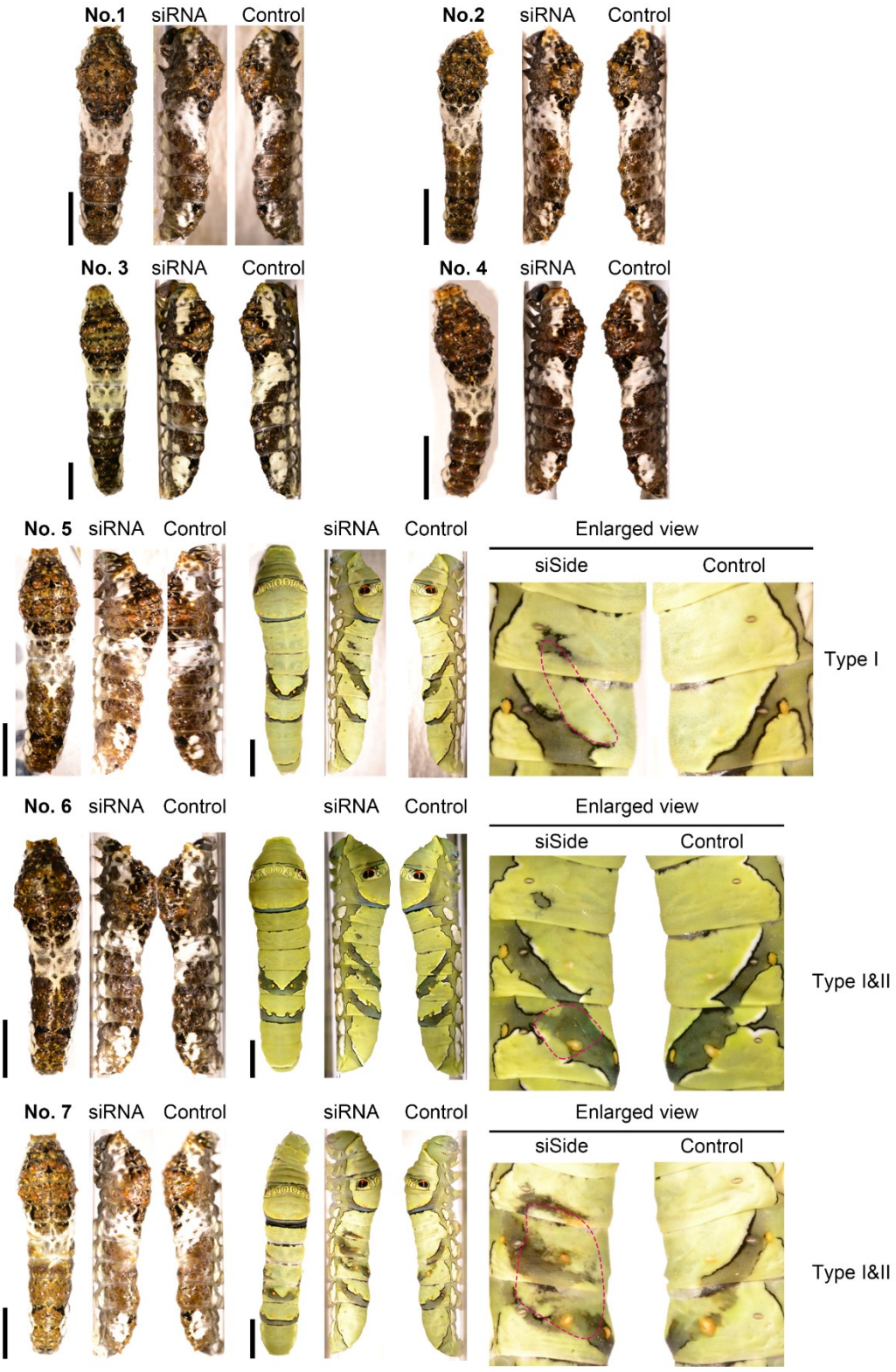

Figure S6. RNAi effects of *Notch*, related to Figure 4. *Notch* siRNA was injected at the 3rd stage and observed at 4th and 5th stage. The type I means that the PSB drop (RNAi region) was placed in the green area around A3 and A4. The type II means that the PSB drop (RNAi region) was placed around the future V-shaped marking around A3 to A5. No. 12 individual shows the *Notch* RNAi effect on A1 segment. Pink dashed circle shows the RNAi region. Scale bar: 5 mm

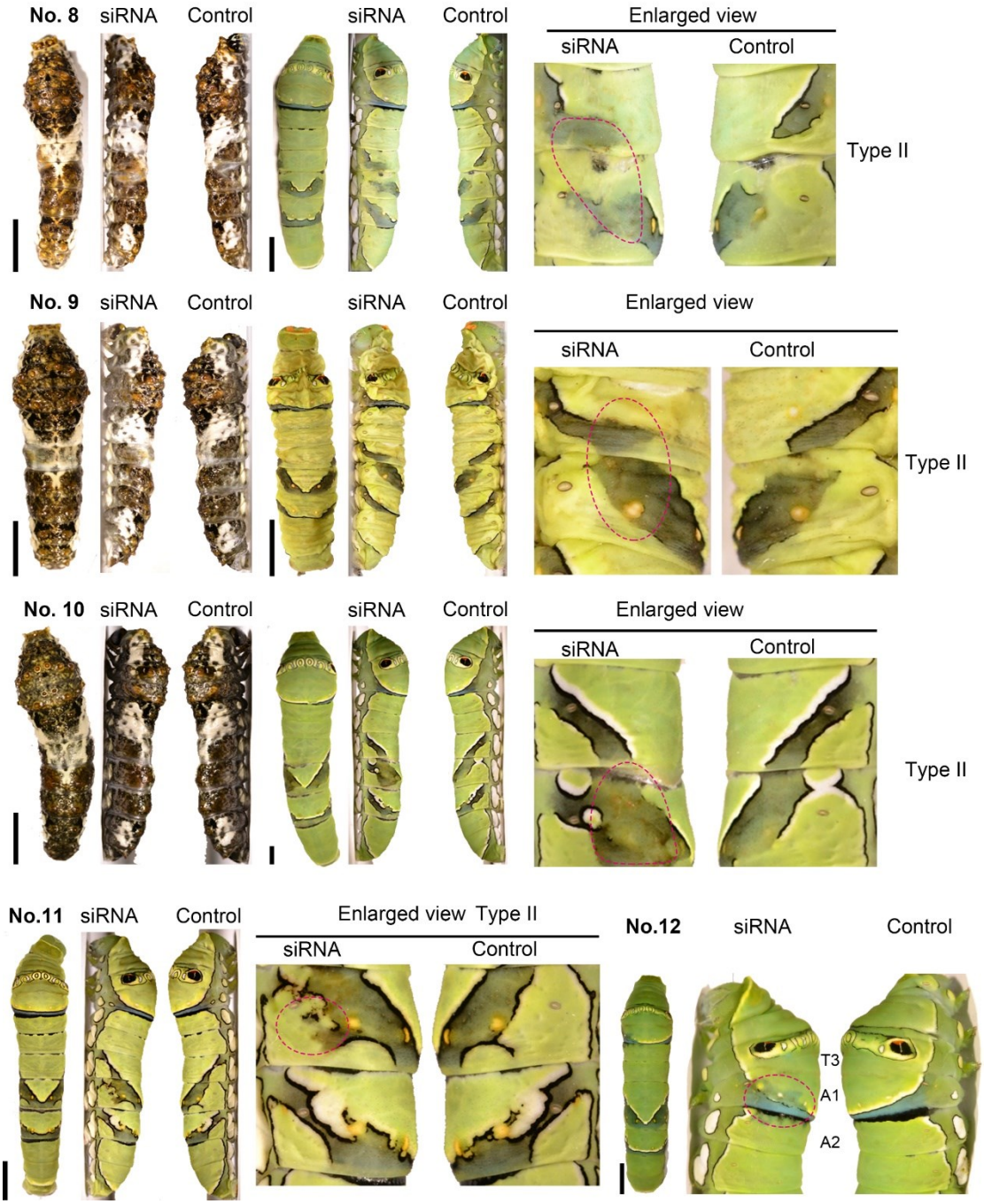

Continued Figure S6. RNAi effects of *Notch*, related to Figure 4.

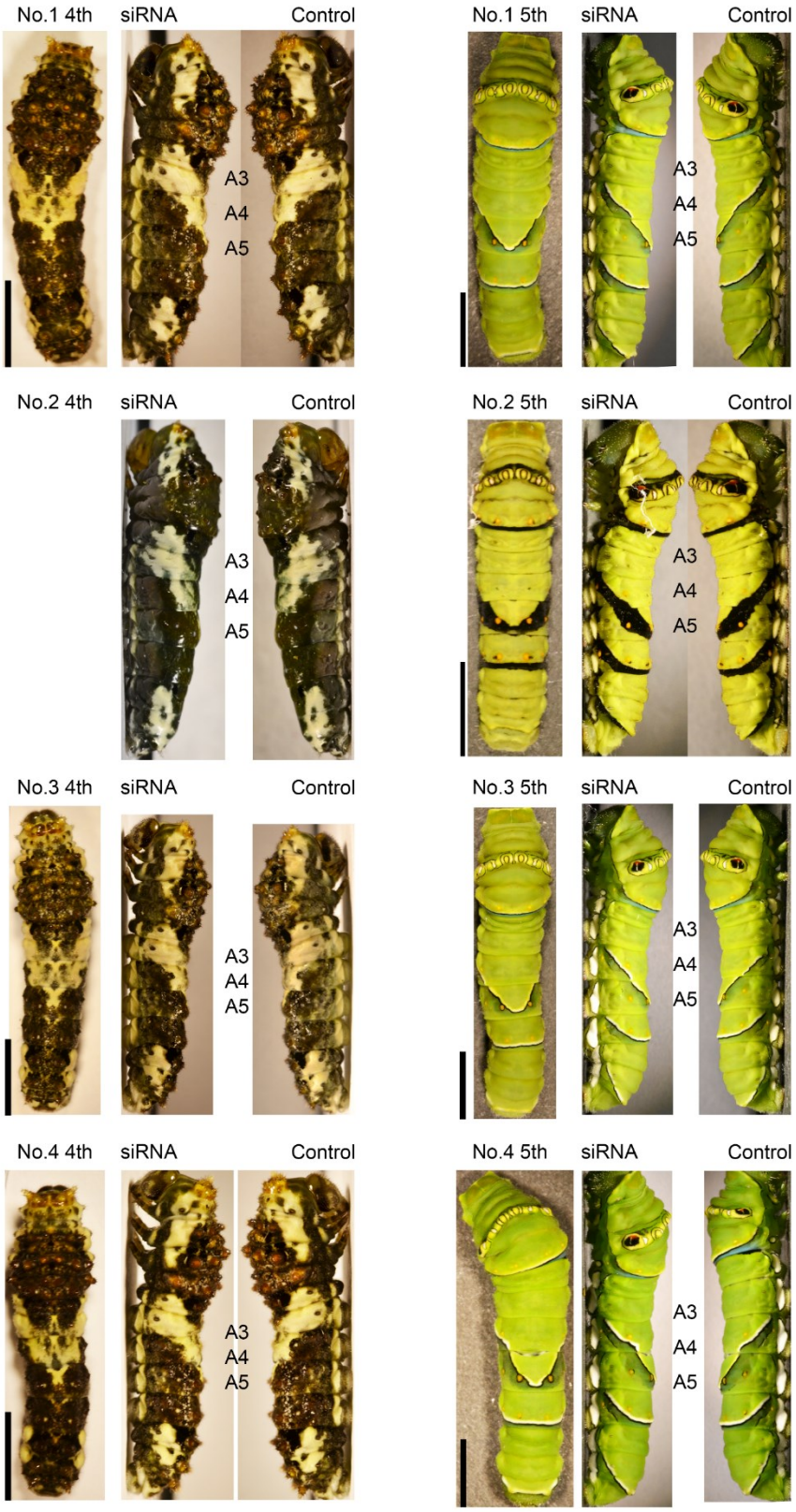

Figure S7. RNAi effects of *Serrate*, related to Figure 3 and 4. *Serrate* siRNA was injected at the 3rd stage and observed at 4tg and 5th stage. No phenotypic changes were observed. The PBS drop (RNAi region) was placed around the green region and future V-shaped marking from A3-A5. Scale bar: 5 mm.

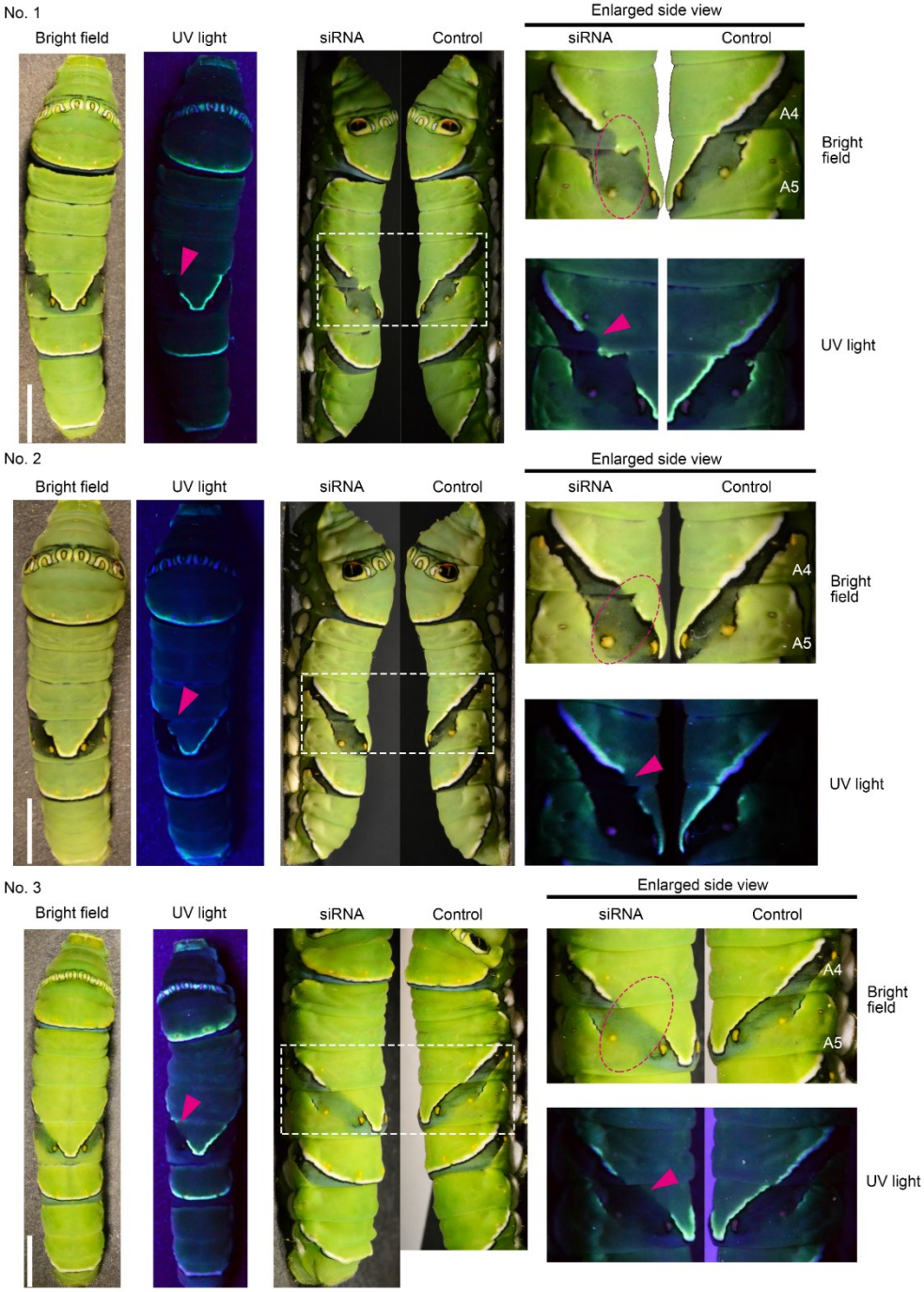

Figure S8. RNAi effects of *Delta*, related to Figure 3. *Delta* siRNA was injected at the 4th stage and observed at 5th stage under bright light and UV light. The PBS drop (RNAi region) was placed around the green region and future V-shaped marking from A3-A5. The pink arrowhead shows the removal of fluorescent on border line. Scale bar: 5 mm.

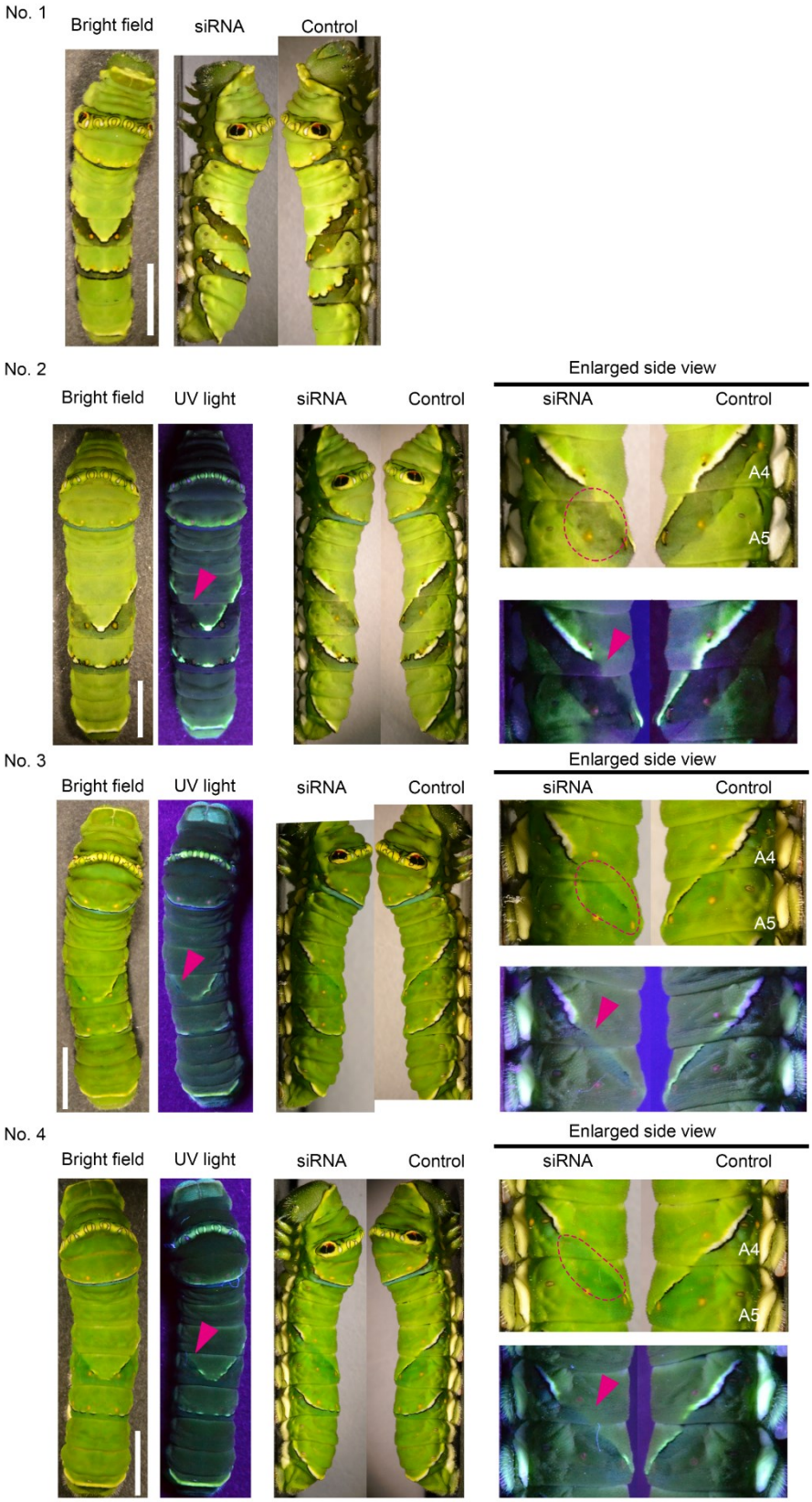

Figure S9. RNAi effects of *Notch*, related to Figure 4. *Notch* siRNA was injected at the 4th stage and observed at 5th stage under bright light and UV light. The PBS drop (RNAi region) was placed around the green region and future V-shaped marking from A3-A5. The pink arrowhead shows the removal of fluorescent on border line. Scale bar: 5 mm.

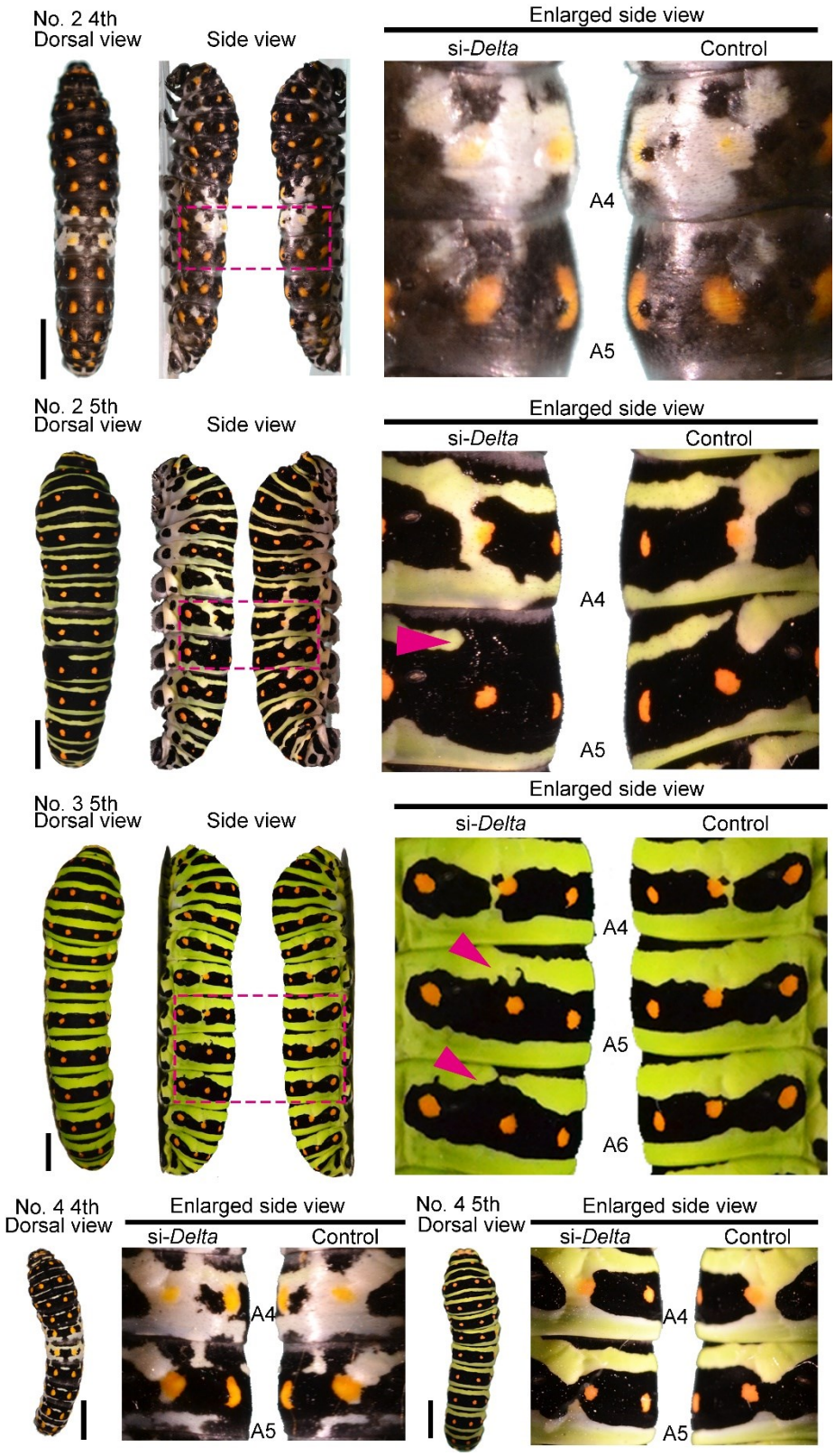

Figure S10. RNAi effects of *Delta* on 4th and 5th instar larvae of *P. machaon*, related to Figure 5. RNAi was performed at late 3rd instar stage. The pink arrowhead shows the ectopic of black pigmentation. Scale bars: 5 mm.

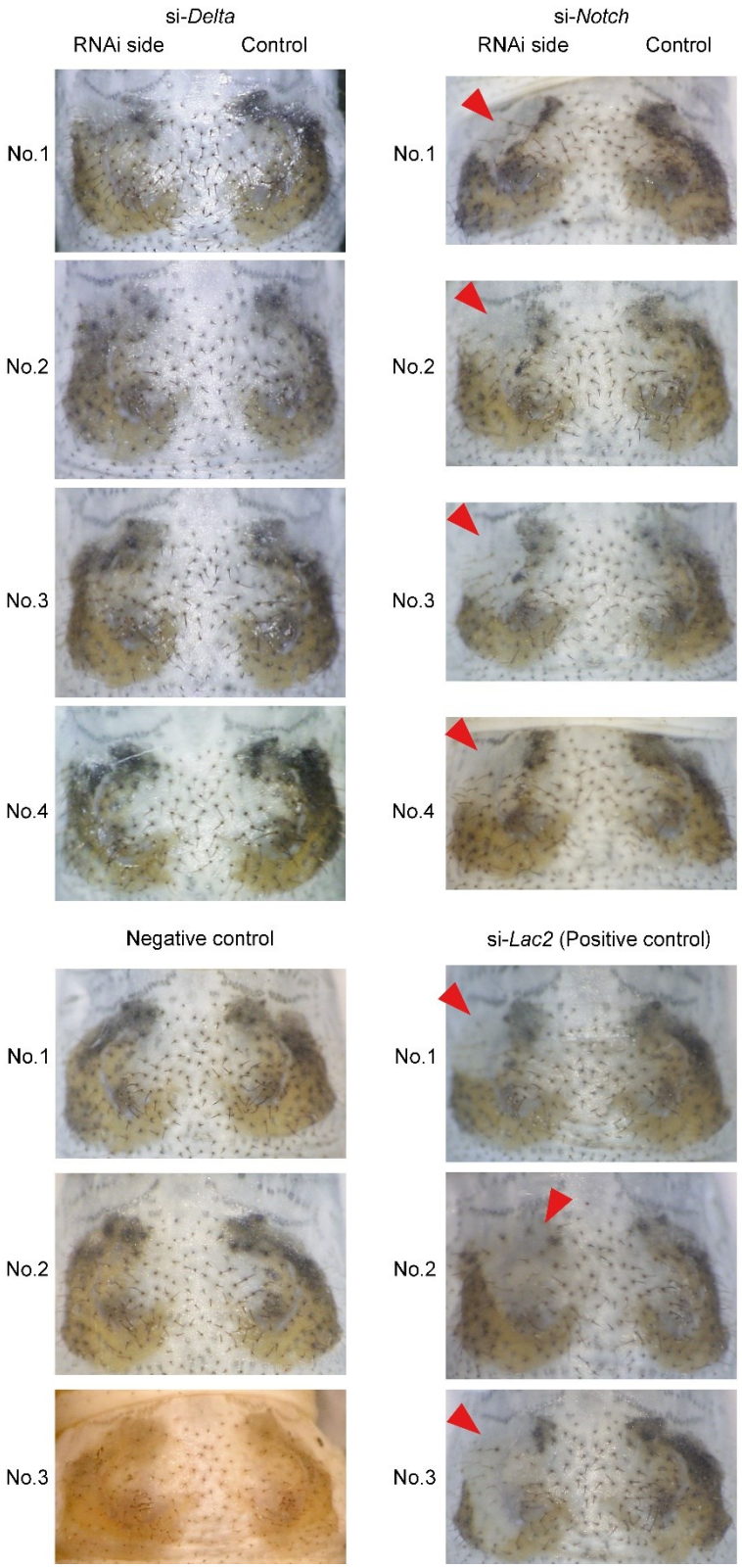

Figure S11. RNAi experiments of *L* mutant, related to Figure 5. RNAi was performed on A2 segment during the intermolt period in 4th instar stage. No phenotypic changes were observed in *Delta* RNAi (n = 3, up left panel) and negative control group (n = 3, down right panel). RNAi of *Notch* inhibited black pigmentation in all individuals (n = 5, up left panel shows individual No.1 -No.4. No.5 is displayed in Fig. 4.5). Pigmentation gene *Lac2* was used as positive control (n = 3, down left panel). Melanization was blocked after RNAi of *Lac2* in all individuals (red arrowheads).

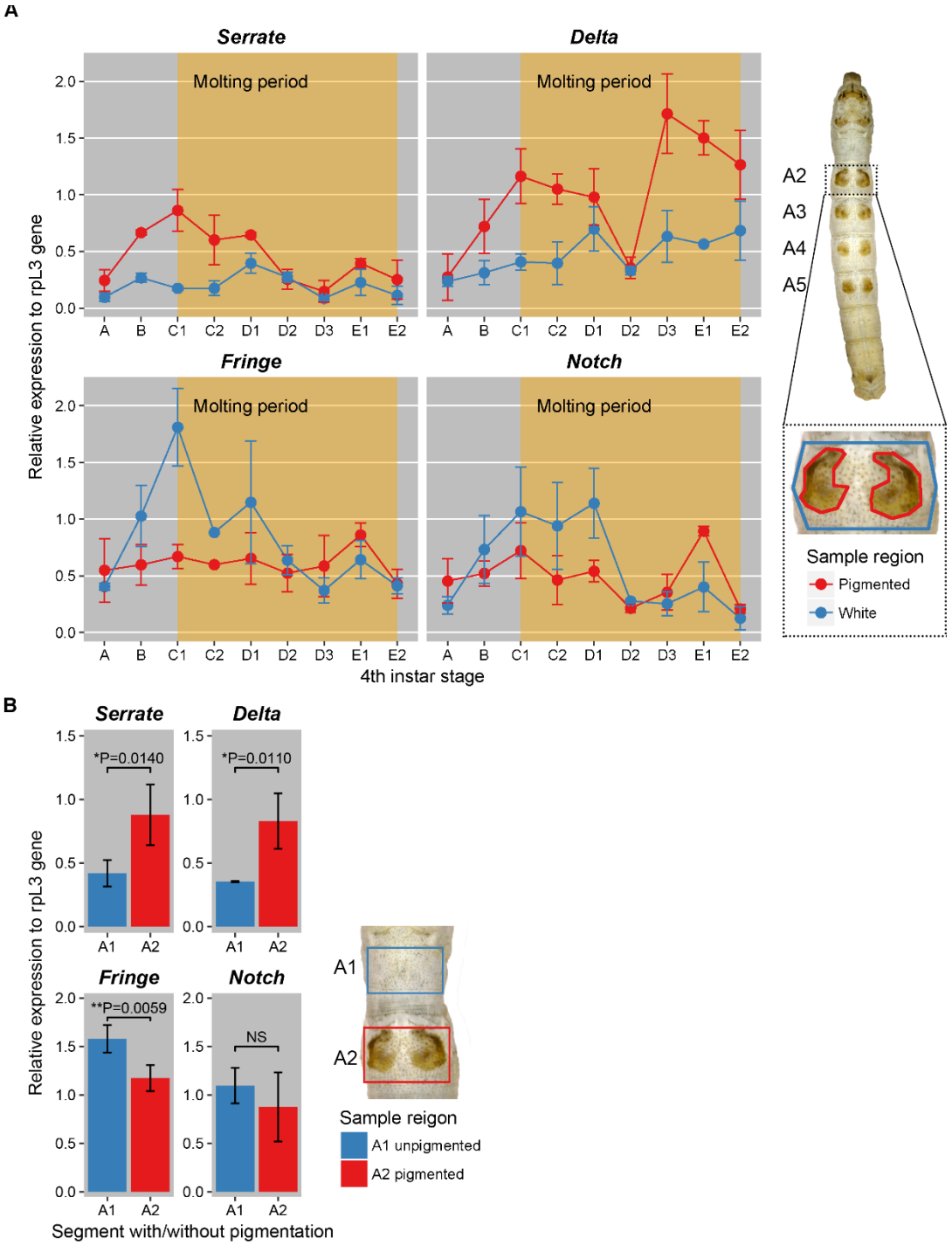

Figure S12. Temporo- and spatial- expressions of Notch related genes in *L mutant* larva using qPCR, related to Figure 5. (**A**) Relative expressions were plotted as means +/- s.d. Epidermis samples were prepared in two regions on A2 segment of 4th instar stage. Sampling stages were based on the description in reference Kiguchi et al., 1983. Molting period indicates the increment of ecdysone titer based on reference Yamaguchi et al, 2013. Red line chart with dots: expression in pigmentated region. Blue line chart with dots: expression in the white region. HCS is around the D2 stage. For stage C1 and D3, n = 4; for the rest stages, n =3. *rpL3* gene was used as internal control. (**B**) Expression of Notch related genes between A1 (blue bars, unpigmented), and A2 (red bars, pigmented) regions at C1 stages were plotted as means +/- s.d. Student' t test was applied. NS: no significant difference.

Transparent Methods

Experimental Animal

P. xuthus eggs were purchased from Mr. S. Shimizu, and wild larvae were collected from a field near the Kashiwa campus of the University of Tokyo. Purchased eggs were reared on an artificial diet, while wild larvae collected from the field were reared on the leaves of *Citrus unshiu* (Rutaceae), at a temperature of 25°C under long-day conditions (at 16 h of light and 8 h of dark). Larvae were reared in a plastic Petri dish (Inner Diameter 90 mm × Height 20 mm, As One Co., Osaka, Japan) for the 1st through to the 4th instar, and the 5th instar larvae were reared in a plastic container (Inner Diameter 125 mm × Height 100 mm, Mineron Kasei Co., Ltd, Osaka, Japan). Larvae of *P. machaon* were collected in a field near the Kashiwa campus of the University of Tokyo. The larvae fed on the plant ashitaba *Angelica keiskei* leaves and kept at a temperature of 25°C under long-day conditions (at a period of 16 h light and 8 h of dark). The *L* mutant (g03) of the *B. mori* was obtained from Kyushu University, Japan. Larvae of *B. mori* fed on mulberry leaves and were kept at a temperature of 20°C under long-day conditions (at a period of 16 h light and 8 h of dark).

The end of larval ecdysis was considered at 0 hour for each stage of development. The staging of the molting period was based on the timing of the HCS. For *B. mori*, precise developmental stages were used according to Ref. Kiguchi, 1983.

Epidermal Sample Preparation, RNA Isolation, and cDNA Synthesis

Larvae of *P. xuthus* and *B. mori* were firstly anesthetized on ice and then dissected. Muscles and fat body were carefully removed and its epidermis was cut along the color patterns. RNA was extracted using TRI reagent (SIGMA), purified and then the concentration was determined using a NanoDrop 1000 spectrophotometer (Thermo Fisher Scientific Inc., USA). Complementary DNA was made by reverse-transcription with random hexamers by a verso cDNA Synthesis Kit (Thermo Fisher Scientific Inc., USA).

Gene Sequence and Primer Design for Quantitative PCR (qPCR)

Primers used for the qPCR technique were designed using the latest version of the Primer3Plus (https://primer3plus.com/). qPCR primers were designed in line with the manuscript of Power SYBR® Green Master Mix (Applied Biosystems, Thermo Fisher Scientific Inc., USA). Primers were designed on neighboring exons resulting PCR product covering two exons that lead to the specific detection of each target gene. Gene sequences used for primer design were obtained from the previous transcriptome database of *P. xuthus* PapilioBase (see Ref. Nishikawa et al., 2015); and is available on http://download.lepbase.org/v4/sequence/).

For *P. xuthus*, *Delta* (PapilioBase gene ID: PxGene7446), *Notch* (PxGene7219) were used. Primers of *Px-Delta*: 5′- CCAGTGTTGGGAGGCAACTC-3′ and 5′-CCACGCTTCGACAATCAGC-3′; of the *Px-Notch*: 5'-ACACGAGTCCTATCAACGGTTC-3' and 5'- GTTCGCATGGAGAACCTTGTTC-3' were used.

For *B. mori*, homologs of *Delta* (BMgn010195), *Serrate* (NM_001309558), *fringe* (BMgn006892), and *Notch* (BMgn007929) gene were manually compared using BLAST against KAIKOBASE (ver.3.2.2, http://sgp.dna.affrc.go.jp/KAIKObase/) or nucleotide collection database from NCBI with E value < 1×10^{-6}. *Fringe* gene sequence (NM_001123341) was obtained according to previous study.

Primers of *Bm-Delta*: 5′- ATCGTGTTCCCCTTCGACTTC-3′ and

5′- TGGATGTGTCGTTGTTGTCG-3′; of the

Bm-Notch: 5'-AAACTGACGTCGATGAGTGC-3' and
5'-AGCCATTGACGCAAATGCAG-3'; of the
Bm-Fringe: 5′-ATGACCGGTTTCTCGAGAGTG-3' and
5'-TTGTAGCACGCTCACCAAAC-3'; of the
Bm-Serrate: 5′-TAAACACGGCTACTGCAACG-3', and
5′-GGGTGCCGCAGTAGTTTAAATC-3' were used.
Internal control of a *ribosomal protein L3* (*rpL3*) gene was introduced to compare the relative expression of targeting gene in both *P. xuthus* and *B. mori*. Primer set of *Px-rpL3* gene was:
5′-CTGGGCGGAGCATATGTCTGAAG-3′ and
5′-TCTTACTGGCTTTAGTGAAAGCCTTCTTC-3';
Of *Bm-rpL3* gene are 5′-CTGGGCGGAGCATA TGTCTGAAG-3′ and
5′-TCTTACTGGCTTTAGTGAAAGCCTTCTTC-3′.

Quantitative PCR Reaction and Measurement of the Relative Gene Expression
Quantitative PCR reaction was performed using Power SYBR® Green Master Mix (Applied Biosystems, Thermo Fisher Scientific Inc., USA) on StepOne Real-Time PCR System and QuantStudio 3 Real-Time PCR System (Thermo Fisher Scientific Inc., USA). For a single color region, relative expression of a target gene was evaluated by (target gene expression) / (*rpL3* expression).

Double Stranded RNA (dsRNA) Design and Electroporation-Mediated RNAi
DsRNAs for RNAi in *P. xuthus*, *P. machaon* and *B. mori* larvae were designed using siDirect (version 2, http://sidirect2.rnai.jp/). The siRNA targeting sequences were as follows:
P. xuthus, *Delta*: 5'- CGACAATCAGCGAGAAAGTGC-3';
Notch: 5'- GGTGTAGAAAGTGACATGATC-3' or
5'- GCATGACATACCAGTATATCC-3';
P. machaon, *Pm-Delta*: 5'- CGACAATCAGCGAGAAAGTGC-3';
B. mori, *Bm-Delta*: 5'-GCACTTTCTCGCTGATTGT-3';
Bm-Notch: 5'-CACCTAAACCCTTGTCATA-3';
Bm-Serrate 5'-CTAACAACCTTCAAAACGA-3';
Bm-Fringe 5'-CAAGATTACCGATCATCTT-3';
Bm-Lac2: 5'-TCTTAATACCACATTCTCCAA-3'.
For *P. xuthus* and *P. machaon*, details of microinjection of dsRNA and electroporation were described in the previous study (see Ref. Jin et al., 2019). For *P. xuthus* and *B. mori* the negative control used for its analysis was a commercial product Universal Negative Control (Nippon Gene Co., Ltd.). One microliter of 250 μM siRNA was injected at the intersegmental membrane between the 7th and 8th abdominal segment into the hemolymph. The electroporation was set to 15 V lasting 280 ms for 5 repeats.

Data Collection and Fluorescent Imaging
A Nikon D3100 with an AF-S DX Micro NIKKOR 85 mm f/3.5G ED lens was used for data collection. A standard setting of F/40, 1/50 s, and ISO 3200 for bright-field photographs and F/32, for 0.62 s and ISO 3200 for fluorescent photographs were used. An Olympus LG-PS2 was set as the main light source for bight filed photography. A LED375N-100STND stand light (Nichia

Corporation), emitting at a maximum of 385 nm UV light, was arranged in a distance of 150 mm from the caterpillar as the only light source for photography.

Quantification and Statistical Analysis

Statistical analyses were performed in Microsoft Excel and online web statistical calculators (https://astatsa.com/). Significance of differences was determined with Student's t test analysis, or one-way ANOVA with subsequent Tukey HSD test.